Electrowetting 2018

The 11th International Conference on Electrowetting and Drop Dynamics on Functionalized Surfaces

18-20 June 2018

University of Twente

Enschede, the Netherlands

ABSTRACT BOOK

Electrowetting 2018

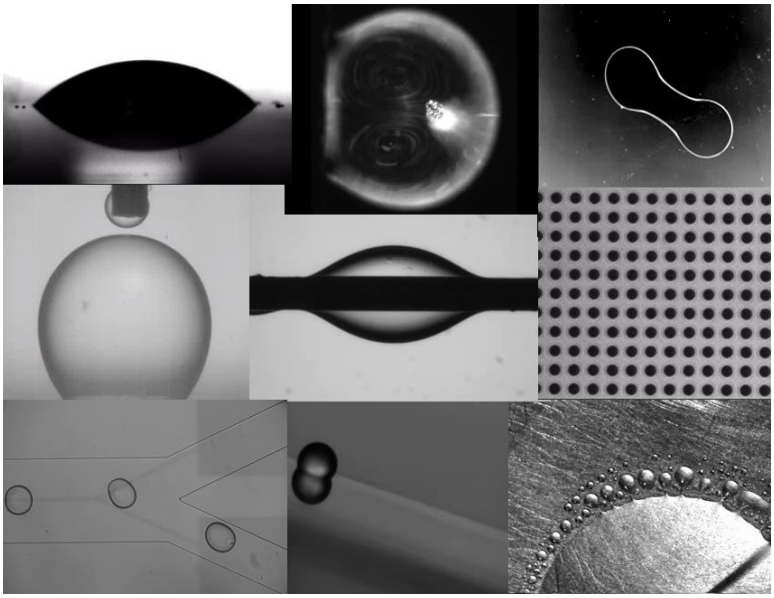

UNIVERSITY OF TWENTE
Enschede, the Netherlands

List of contents:

Invited speakers

Jean-Christophe Baret

University of Bordeaux, CRPP-CNRS, France

Burak Eral

Delft University, the Netherlands

Michael Dickey

North Carolina State University, United States

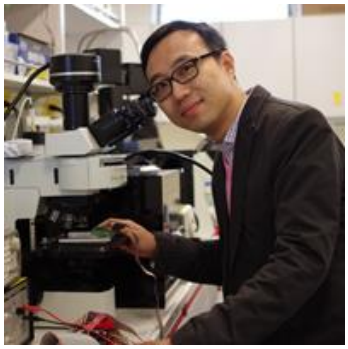

Shih-Kang "Scott" Fan

National Taiwan University, Taiwan

Alex Henzen

South China Normal University, China

Alenka Luzar

Virginia Commonwealth University, United States

Jacco Snoeijer

University of Twente, the Netherlands

Hans Zappe

IMTEK, Albert-Ludwigs Universität Freiburg, Germany

Electrowetting and Dielectrowetting on Lubricant Impregnated Surfaces

Glen McHale[1], Zuzana Brabcova[1], Gary. G. Wells[1], Michael I. Newton[2] and Carl. V. Brown[2]
[1]*Smart Materials & Surfaces Laboratory, Faculty of Engineering & Environment, Northumbria University, Newcastle upon Tyne, NE1 8ST, UK*
[2]*School of Science and Technology, Nottingham Trent University, Nottingham NG11 8NS, UK*

Electrowetting is limited by the extent to which it can induce the complete spreading of a liquid over an otherwise non-wetting substrate due to the well-known saturation effect. It is also subject to contact angle hysteresis associated with pinning forces at the contact line. In recent work, we have shown that interface localized liquid dielectrophoresis (dielectrowetting) can induce a droplet to spread into a film [1], thus addressing the first limitation of electrowetting. At the same time, there have been significant advances in the literature in producing lubricant impregnated (LI), or equivalently slippery liquid infused porous (SLIP), surfaces which almost eliminate the contact angle hysteresis suffered by droplets. The LIS/SLIPS idea has previously been applied to create a completely reversible and tunable electrowetting-based liquid lens with improved transient response due to reduced droplet oscillations [2]. However, that work did not consider the limitation from contact angle saturation. In this work, we consider the use of dielectrowetting to axisymmetrically spread a droplet in a controllable and hysteresis-free reversible manner on a non-wetting surface. For comparison, we also consider the electrowetting of droplets on identical SLIP surfaces [3]. In the case of electrowetting we observe a complete removal of hysteresis for voltages above the saturation contact angle voltage. In the case of dielectrowetting, the contact angle hysteresis is reduced to less than 4° whilst retaining the ability to fully spread a droplet into a liquid film. In both cases, the cosine of the contact angle retains a quadratic dependence on applied voltage, consistent with previous theoretical expectations. We show that data for both electrowetting and dielectrowetting can be scaled onto a universal curve by choice of an initial contact angle at zero applied voltage and a threshold voltage for film formation extrapolated from each data set (Fig. 1). Our studies show that fully reversible spreading encompassing a wide range of partial wetting droplet states and a film state can be achieved in air in a controllable manner with very low levels of hysteresis by the use of lubricant impregnated substrates. Since the dielectrowetting approach can achieve reversible low hysteresis control between a droplet and a film state in air without mechanical parts and in a scalable manner, it may be significant for a range of applications, including liquid-based optics and droplet-based microfluidics.

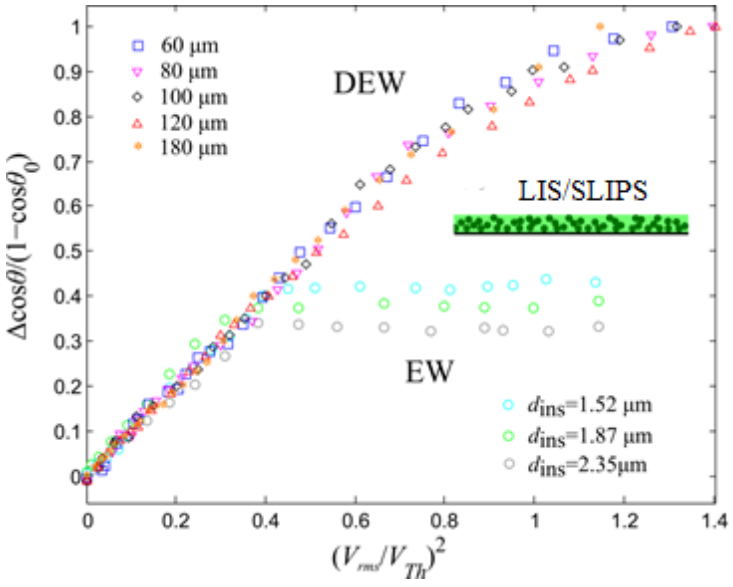

Figure 1. Data scaled onto a universal equation using the initial contact angle θ_0 and threshold voltage, V_{Th}, for film formation.

Acknowledgements. We would like to thank Dr Michael Cooke, Dr Pietro Maiello, Dr Edward Bentley, Dr Ben Xu and Dr. Andrew Edwards for valuable advice and technical support. This work was financially supported by the UK Engineering & Physical Sciences Research Council (EPSRC grants EP/K014803/1 and EP/K015192/1).

References

[1] G. McHale, C.V Brown, M.I. Newton, G.G. Wells, and N. Sampara. Physical Review Letters **107**, 186101 (2011).
[2] C. Hao, Y. Liu, X. Chen, Y. He, Q. Li, K.Y. Li, and Z. Wang. Scientific Reports **4**, 6846 (2014).
[3] Z. Brabcova, G. McHale, G.G. Wells, C.V. Brown, and M.I. Newton. Applied Physics Letters **110**, 121603, (2017).

Forming fluids to focus photons

Hans Zappe

Gisela and Erwin Sick Chair of Micro-optics, Department of Microsystems Engineering,
University of Freiburg, Georges-Koehler-Allee 102, 79110 Freiburg, Germany

Electrowetting as a means to form fluid surfaces has played a major role in optofluidics, in which fluid surfaces are used to dynamically modulate optical fields. Optofluidic optical systems have been developed for a wide variety of applications, including tunable lenses; fluidic waveguides; optical switches; liquid lasers; and tunable apertures. For the classical optical engineer, however, optofluidic devices have only had limited relevance, since optical imaging systems require components delivering high imaging quality and controlled aberrations. To address these issues, our recent work on fluidic optical components has yielded liquid-based micro-optical imaging systems which demonstrate tunability, ultra-compact design, and viability for real optical imaging applications.

We will present new concepts in aberration-controlled, multi-element tunable optofluidic devices and systems which advance the state-of-the-art in ultra-miniaturized tunable and adaptive optics. By combining concepts and technologies from micro-fluidics, micro-optics and micro-fabrication, a three-dimensional fluidic system has been realized inside a cylinder, as seen in Figure 1, using complex electrode patterns on its inner surface for highly-flexible electrowetting actuation. A variety of density-matched, immiscible liquids with optimized refractive and dispersive properties, all individually tunable, fills the tube and is used to generate a variety of optical functions. These include individual and multiple tunable lenses; astigmatism-tunable optics; variable and rotatable prisms; tunable apertures; and an all-fluidic zoom system, all with excellent imaging properties. These developments pave the way for the use of optofluidics in an increasingly broad spectrum of imaging applications.

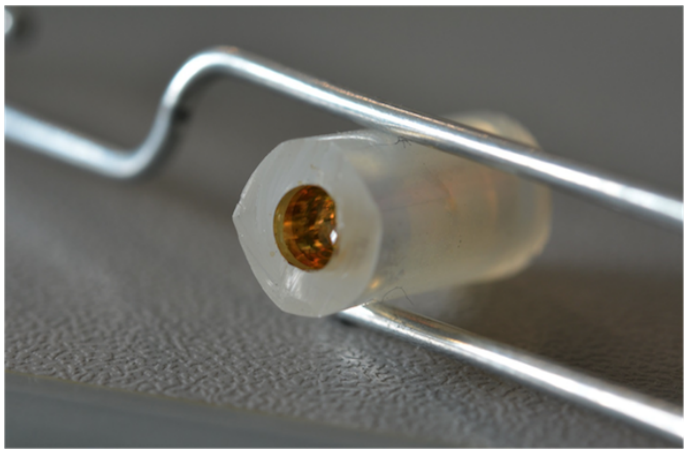

Figure 1: A complete electrowetting-actuated fluidic optical zoom system in a tube.

Topic no. XX (see website/flyer)
Oral or poster EW Conf. 2018

Title: EWD technology for electronic Changeable Copy Boards

Hans Feil
Etulipa

Light pollution and energy consumption prohibit that LED displays become as abundant as "paper". Electro-wetting displays can fullfil that role, because of their highly reflective performance. Etulipa Carbon is the first electro-wetting product going to market that successfully passes all perception tests on readability under all outdoor conditions.

Etulipa has chosen to focus upon on-premise electronic changeable copy (eCCB) boards as first product to the market. The first product introduction of the Etulipa Carbon enables business owners in residential area's, to easily get permits for placing digital displays, and operate such digital displays with extremely low energy consumption. In fact, it can be run off-grid using a battery or solar-energy based solution.

End of 2017 Etulipa started the production of display tiles in Taiwan. Eight of those tiles are combined into panels and 15 panels are combined into one screen. Short movies of the production line and of the eCCB will be shown.

Among the biggest challenges is to make the displays work reliably at very low and high temperatures, under bright sunshine and for long periods. A few of the materials science challenges will be discussed.

Figure 1 eCCB prototype

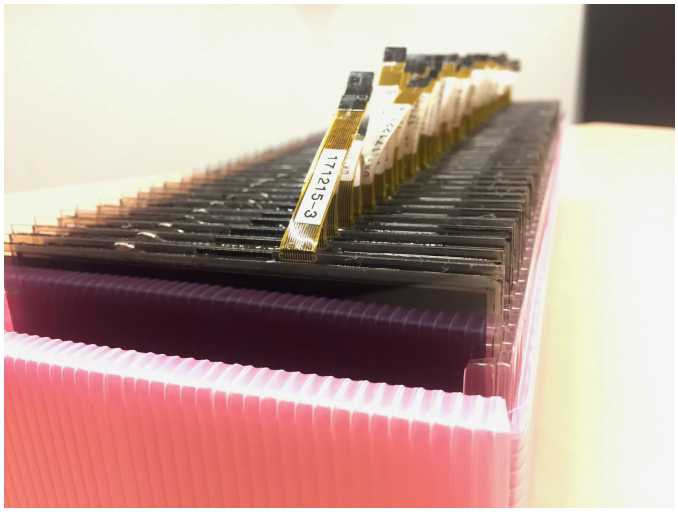

Figure 2 EWD tiles ready for panel assembly

Creation of aspherical surfaces on a liquid lens

Matthias Strauch, Peter A. A. M. Somers, and H. Paul Urbach
Delft University of Technology (Netherlands)

Since electrowetting liquid lenses have been developed, fast focal switching has merely been considered being a source of aberrations and a loss of imaging quality [1]. The stimulated creation of surface waves on a liquid lens has only recently shifted into the focus of research in cryptographic imaging and been studied in more detail [2-3]. This work focuses on how to create aspheres on a liquid lens using an AC voltage actuation signal.

In previous studies [3] it has been demonstrated, that surface waves on a liquid lens surface can be described by Bessel functions $J_0(x)$. The approximation is valid for small surface deviations and frequencies. Scaled Bessel functions are orthogonal and therefore allow the description of any radially symmetric surface function $u(r)$ as a sum of Bessel functions

$$u(r) = \int_0^\infty A(f)\, J_0\left(\frac{2\pi f}{c} r\right) \mathrm{d}f$$

where f is the frequency, r is the radius, and c is the speed of wave in the approximation of the model. The desired surface shape can be obtained by determining the coefficients $A(f)$. This is realized by using a Hankel transform:

$$H_0(k) = \int_0^\infty u(r)\, J_0(kr)\, r\, \mathrm{d}r$$

The inverse Fourier transform of the coefficients $A(f)$ yields the time dependent voltage actuation signal, that is necessary to create the desired surface at time $t = 0$.

The used liquid lens is an Arctic39N0 by Varioptic. The surface shape is measured with a Mach-Zehnder interferometer. The interferogram is analysed using Fourier transforms and phase unwrapping to obtain the surface profile.

An application of this technique is the creation of a Zernike polynomial on the liquid lens surface (see figure). The shown Zernike surface can be used to correct the spherical aberration of another optical system, or just the aberration of the liquid lens itself. The converted time-dependent voltage signal is pulsed due to the finite extensions of the liquid lens. The calculated signal can then be added to a flat or spherical lens surface.
The interferometric measurement shows a nice agreement between the desired and the created Zernike polynomial. For large radii the surface values stay slightly below the Zernike functions due to the limitations of the model for high frequency actuation.

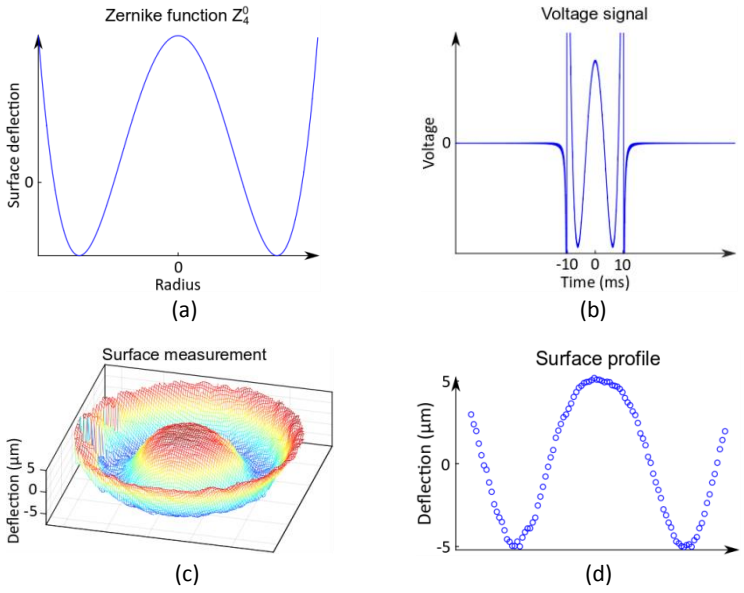

A spherical aberration is created on the liquid lens to test the applicability of the model. The Zernike polynomial is displayed in figure (a). The calculated actuation voltage input for the liquid lens is shown in figure (b). The surface reconstruction based on interferometric measurements is shown in figure (c) and the surface profile is displayed in figure (d).

Conclusion

It is possible to design aspheric lens surface shapes using of-the-shelf liquid lenses. While it is theoretically possible to create any surface shape by superposition, in practice the shapes are limited by the frequency response of the liquid and the simplifications of the surface model.

References

[1] S. Kuiper and B. H. W. Hendriks, Appl. Phys. Lett. **85**, 1128 (2004)
[2] D. R. Schipf and W.-C. Wang, Proc. SPIE **10559**, 1055908 (2018)
[3] M. Strauch, Y. Shao, F. Bociort, and H. P. Urbach, Appl. Phys. Lett. **111**, 171106 (2017).

Particle assisted electrowetting driving multiway optical valves

Lin Chen[1,2] Mingliang Jin[1,2], Guofu Zhou[1,2], and Lingling Shui[1,2*]

1 National Center for International Research on Green Optoelectronics, South China Normal University, Guangzhou 510006, China

2 Guangdong Provincial Key Laboratory of Optical Information Materials and Technology and Institute of Electronic Paper Displays, South China Academy of Advanced Optoelectronics, South China Normal University, Guangzhou 510006, China

Abstract

We report on a high efficiency and position controllable multiway optical valve achieved by electrowetting (EW) driven and magnetic particle directed oil film dewetting in a microscale space. Under the same working conditions, with introducing a magnetiv particle, the valve's opening voltage can be decreased from 24 V to 10 V, and its opening ration can be increased from 65% to 75%. A 16-way spatial valve has been achieved in single microspace.

Context

Dewetting phenomenon is very important in practical applications like marine oil drilling, underwater coatings for ships or cables[1]. The surface wettability change by electrowetting can be considered as a wetting and dewetting process, which can be widely applied in microfluidic manipulation for microlens, displays and optical switches [2-4]. In this work, we constructed an electrowetting device with a comparable structure by placing a thin dielectric oil film between upper conductive water and bottom electrode. The oil film dewets and breaks driven by electrowetting with the determinative parameters of electric field and film thickness. With introducing an extra MP in the device, the oil film thickness distribution is then rearranged. Thus, the dual water (hydrophilic)-oil (oleaphilic) interface can be well guided by either a hydrophilic MP (HMP) or an oleaphilic MP (OMP) to break and move to designed direction and location. In this way, the spatially multiway valves can be achieved by electrowetting actuating and MP guiding microfluidic flow. The optical performance of these valves like switching speed and opening ratio is improved compared to those without a MP. As shown in Figure 1, the oil film distribution and resulted oil film dewetting and opening direction are well tuned.

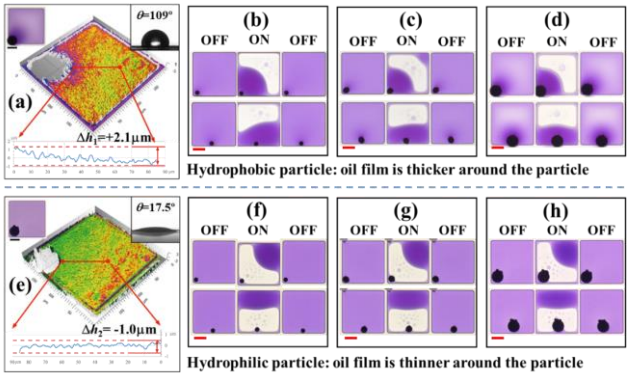

Figure 1. Oil distribution in microwells. (a) and (e) The 3D image of the oil film distribution with a 50 μm OMP and HMP in a microwell, respectively. Insets are the microscopic optical image and the measured contact angle. (b-d) EW driven Off-On-Off phenomenon in microwells with 15, 30 and 50 μm OMPs in the microwells, respectively. The OMPs are located at a corner (top) or in the middle of a wall (bottom). (f-g) are the HMPs in microwells with the same size and position as the OMPs.

Results and Conclusions

A high efficiency and well-controllable EW optofluidic modulation has been demonstrated by introducing a MP in a dual fluidic micro-area. The spatially controllable EW driven switching is determined by the surface wettability, location and size of the MPs. Switching on voltage (V_{open}) from 24 V to 10 V and the maximum opening ratio (OR_{max}) from 65 % to 75 % has been achieved by introducing a 10 μm OMP in a 185×185×6 μm^3 microwell. 16-way spatial valve has been achieved by moving one MP in single microwell.

References

[1] S. Herminghaus, Phys. Rev. Lett. **83** (12), 2359-2361 (1999).
[2] P. Mach, T. Krupenkin, S. Yang, and J. A. Rogers, Appl. Phys. Lett. **81** (2), 202-204 (2002)
[3] R. A. Hayes and B. J. Feenstra, Nature **425** (6956), 383-385 (2003)
[4] M. J. Jebrail, M. S. Bartsch, and K. D. Patel, Lab Chip **12** (14), 2452-2463 (2012)

Topic no. 8 Novel Applications
Oral or poster
EW Conf. 2018

EWOD-Aided Droplet Transport on Texture Ratchets

Di Sun[1], and Karl F. Böhringer[1]
[1] *Electrical Engineering Department, University of Washington, Seattle, 98195, USA*

We report a novel droplet transport device using electrowetting-on-dielectric (EWOD) on an open surface with anisotropic ratchet conveyors (ARC). The micro-sized hydrophilic texture on top of a SiN_x and Cytop dielectric layer is successfully achieved by using parylene-C as a stencil mask without degrading Cytop surface properties. 15 μL water droplets are transported with a single sine or square wave electrical signal and without control circuitry for addressing individual electrodes. The average transport speed is 6.6 mm/s under 60 V_{pp} sine wave at 50 Hz.

Water droplets can be transported under orthogonal vibrations with asymmetric ratchet conveyors (ARC), which requires patterning hydrophilic textures on a hydrophobic background [1]. However, patterning on hydrophobic surfaces (like Teflon, Cytop) is difficult using standard photolithography due to poor adhesion between photoresist and substrate. Methods [2]-[3] have been proposed to reduce the surface hydrophobicity but the original surface properties will be damaged. By adopting parylene-C as a stencil mask, we create hydrophilic patterns on top of the Cytop surface without degrading the original surface properties.

The design of the EWOD system with ARC is shown in Fig. 1(A). The center electrode width is 2 mm and the gaps between the electrodes are 50 μm. 220 nm SiN_x and 100 nm Cytop are deposited on top of the electrodes as the dielectric layer. The semi-circular hydrophilic rungs are defined by 50 nm SiO_2 on top of the Cytop, with 10 μm rung width and 50 μm gap between the centers of each rung. The system was fabricated on a 4" soda lime glass wafer. 10 nm Cr and 50 nm Au was patterned to create coplanar electrodes by lift-off. The SiN_x layer was deposited using PECVD and Cytop was spin-coated and cured at 160°C for 1 hour. The wafer was coated with 2.5 μm parylene-C as the stencil mask. 10 nm Al was evaporated on the parylene-C surface as etch stop mask and patterned to define the ARC tracks. The exposed parylene-C area was etched with RIE, followed by 50 nm SiO_2 with e-beam evaporation. The parylene-C layer was carefully peeled off using tweezers before further testing.

AC signals were provided by a function generator and amplified by a voltage amplifier with the factor 200 V/V. A water droplet was pipetted and the droplet silhouette was monitored by a high-speed camera. For the dynamic water droplet transport characteristics, a typical position change of the leading and trailing edge of the water droplet with time is plotted in Fig. 1(B). The leading and trailing edges are three-phase lines (TPL) between liquid, gas and solid, which periodically wet and dewet the substrate due to electrical field oscillation. The leading edge conforms to the hydrophilic ARC rungs, creating a larger TPL line fraction and thus a higher pinning force than the trailing edge, which makes only intermittent contact with the hydrophilic rungs. The anisotropic pinning force causes the water droplet to move forward. Fig. 1(C) shows the top view of two water droplets moving in opposite directions under 20 Hz sine wave signal, demonstrating droplet transportation capability without complex circuitry control.

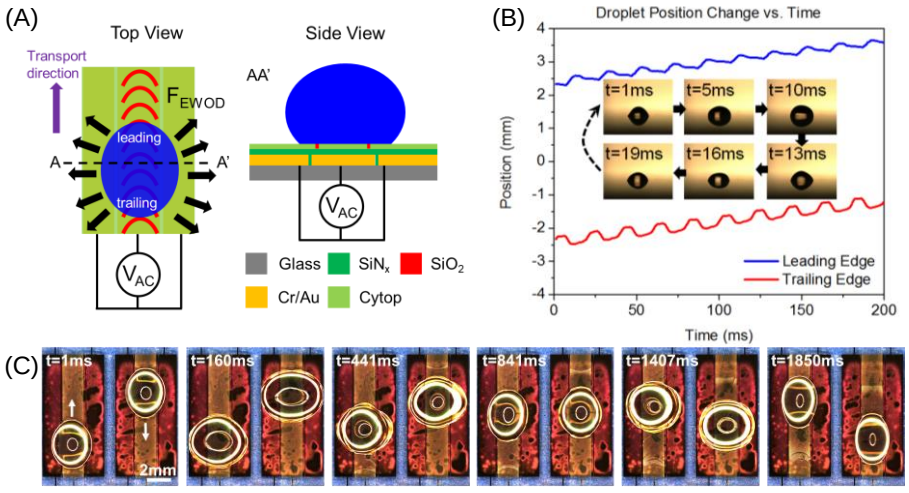

Fig. 1(A) Design of the coplanar EWOD system with ARC texture patterns. The water droplet oscillates due to the EWOD force when an AC signal is applied.

Fig. 1(B) Change in position of leading and trailing edges of a 15μL water droplet with time. The applied voltage was a 60Vpp sine wave at 50Hz. Insets show water droplet silhouettes recorded by high speed camera within one period (20ms).

Fig. 1(C) Top view of the droplet transport under a 20Hz 60Vpp sine wave electrical signal. The two adjacent ARC tracks were designed to transport two droplets in opposite directions at the same time.

References

[1] T. A. Duncombe, J. F. Parsons, and K. F. Böhringer, "Directed drop transport rectified from orthogonal vibrations via a flat wetting barrier ratchet.," *Langmuir*, vol. 28, no. 38, pp. 13765–70, 2012.

[2] S. A. Makohliso, L. Giovangrandi, D. Leonard, H. J. Mathieu, M. Ilegems, and P. Aebischer, "Application of Teflon-AF(R) thin films for bio-patterning of neural cell adhesion," *Biosens. Bioelectron.*, vol. 13, no. 11, pp. 1227–1235, 1998.

[3] C. C.Cho, R. M. Wallace, and and L.A. Files-sesler, "Patterning and Etching of Amorphous Teflon Films," *J. Electron. Mater.*, vol. 23, no. 8, 1994.

Topic no. XX (see website/flyer)
Oral or poster EW Conf. 2018

External-Field-Induced Wetting for Controllable Liquid Transport

Dongliang Tian[1,2], and Lei Jiang[1,2,3]
[1] *School of Chemistry, Beihang University, Beijing 100191*
[2] *Beijing Advanced Innovation Center for Biomedical Engineering, Beihang University, Beijing 100191*
[3] *Technical Institute of Physics and Chemistry, Chinese Academy of Sciences, Beijing 100191, P. R. China*
E-mail: tiandl@buaa.edu.cn

Abstract:
External-field-responsive liquid transport has received extensive research interest owing to its important applications in microfluidic devices, biological medical, liquid printing, separation, and so forth. To realize the different levels of liquid transport on surfaces, the balance of the dynamic competing processes of gradient wetting and dewetting should be controlled to achieve good directionality, confined range and selectivity of liquid wetting [1,2]. Here we will introduce our recent research results on external-field-induced liquid transport on the different levels of surfaces (**Fig. 1**), including directional liquid motion on the surface based on the wettability gradient under an external field [3], partial entry of a liquid into the surface to achieve patterned surface wettability for printing[4-7], and liquid selective permeation of the film for separation [8]. These works are promising to gear up the investigation and application of micro/nanofluidic devices, micro/nanoelectronics, biological and chemical detection and broaden their applications.

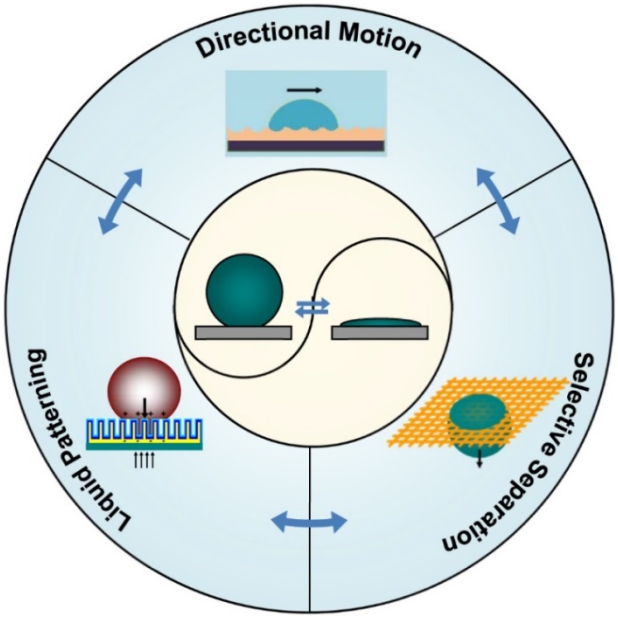

Fig. 1 External-field-responsive liquid transport on the different levels of surfaces owing to the dynamic balance of gradient wetting and dewetting, including directional liquid motion on the surface based on the wettability gradient under an external field, partial entry of a liquid into the surface to achieve patterned surface wettability for printing, and liquid selective permeation of the film for separation.

Reference

[1] Tian, D. L., Song, Y. L. and Jiang, L. Chem. Soc. Rev. **42**, 5184-5209. (2013).
[2] Li, Y., L. He, L. L., Zhang, X. F., Zhang, N. and Tian, D. L. Adv. Mater. **29**, 1703802. (2017).
[3] Tian, D. L., He, L. L., Zhang, N., Zheng, X., Dou, Y. H., Zhang, X. F., Guo, Z. Y. and Jiang, L. Adv. Funct. Mater. **26**, 7986-7992. (2016).
[4] Tian, D. L., Chen, Q. W., Nie, F.-Q., Xu, J. J., Song, Y. L. and Jiang, L. Adv. Mater. **21**, 3744-3749. (2009).
[5] Tian, D. L., Zhai J., Song, Y. L. and Jiang, L. Adv. Funct. Mater. **21**, 4519-4526. (2011).
[6] Guo, Z. Y., Zhang, X. F., Zheng, X., Liu, Z. Y., Cai, J. H., Tian, D. L., Li, W. X., Zhai, J., Song Y. L. and Jiang, L. J. Mater. Chem. A **2**, 2498-2503. (2014)
[7] Guo, Z. Y., Zheng, X., Tian, D. L., Song, Y. L., Zhai, J., Zhang, X. F., Li, W. X., Wang, X. L., Dou, S. X. and Jiang, L. Nanoscale **6**, 12822-12827. (2014).
[8] Zheng, X., Guo, Z. Y., Tian, D. L., Zhang X. F., Li W. X. and Jiang, L. ACS Appl. Mater. Interfaces **7**, 4336-4343. (2015).

Modeling Droplet Dynamics on Liquid Infused Surfaces

Muhammad Subkhi Sadullah[1], Ciro Semprebon[2], and Halim Kusumaatmaja[1]
[1]*Department of Physics, Durham University, Durham DH1 3LE, UK*
[2]*Smart Materials & Surfaces Laboratory, Faculty of Engineering & Environment, Northumbria University, Newcastle upon Tyne NE1 8ST, UK*

Inspired by pitcher plants, Liquid Infused Surfaces (LIS) are constructed by infusing rough or porous materials with a lubricant and they have been shown to exhibit many advantageous surface properties, including self-cleaning, drag reduction, anti-icing and anti-fouling [1]. In this contribution, we demonstrate how our ternary free energy lattice Boltzmann model [2] is suitable for studying droplet dynamics on LIS [3]. First, we find that there is a rich interplay between contact line pinning and viscous dissipation at the wetting oil ridge. As shown in Fig. 1, the effect of contact line pinning is prominent for relatively large apparent contact angle. For lower apparent contact angle, viscous dissipation at the wetting ridge is more important and hence the shape of the wetting ridge, characterised by aspect ratio, is key for determining the droplet mobility. Second, we observe that the advancing mechanism of the droplet is a combination of sliding and rolling motion, and that the amount of rolling is affected by the droplet shape and the contact area with solid. Due to the nature of the corrugated substrate, the solid contact area of the droplet decreases quickly with increasing apparent contact angle. Therefore, droplet on LIS demonstrates different rolling dynamics compared to smooth surfaces.

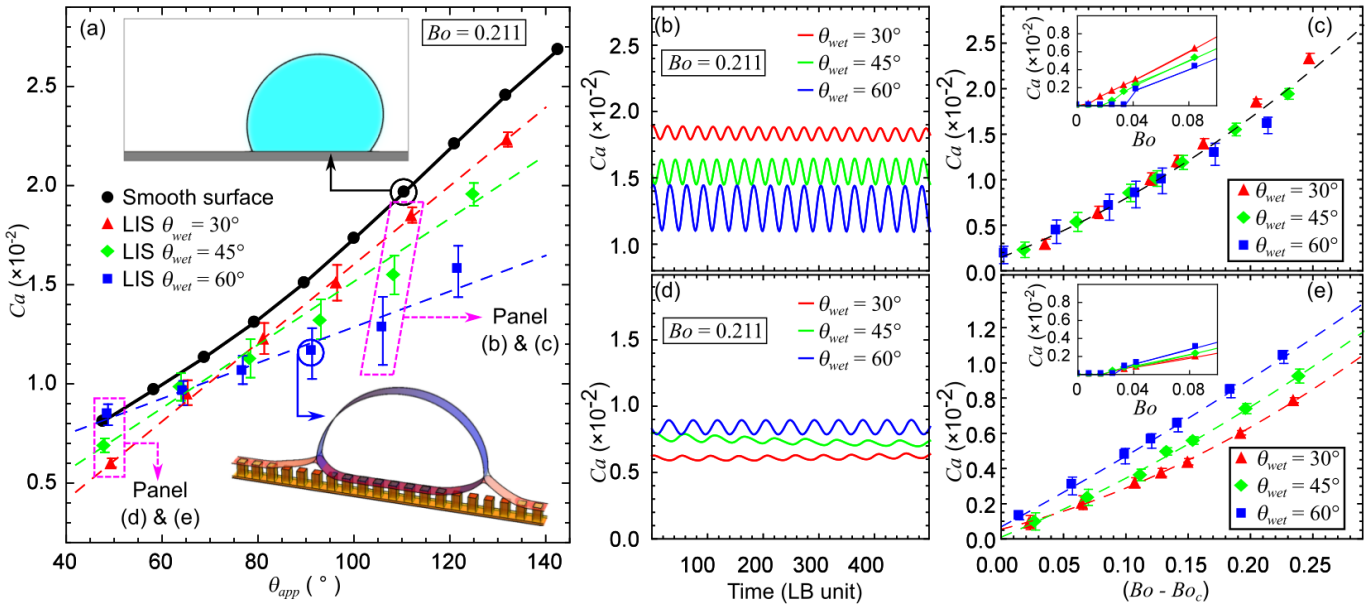

Fig.1 (a) Droplet mobility on smooth surface (black dots) and LIS (red triangles, green diamonds, and blue squares) plotted against droplet apparent angle θ_{app}. θ_{wet} is the contact angle of the lubricant phase in the presence of gas and droplet phase, $\theta_{og} = \theta_{ow} = \theta_{wet}$. The droplet mobility is represented by the capillary number *Ca*. (b) and (d) droplet mobility versus time for the cases indicated in panel (a). The capillary number *Ca* increases and decreases periodically due to pinning-depinning events. (c) and (e) droplet mobility for cases indicated in panel (a) as a function of Bo-Bo_c. Bo is the Bond number. The insets show the critical Bond number, Bo_c, at which the droplets start moving under external body force.

[1] C Semprebon, T Kruger, H Kusumaatmaja, *Phys. Rev. E* **93**, (2016), 033305.
[2] T S Wong et al., Nature **477**, (2011), 443.
[3] M S Sadullah, C Semprebon, H Kusumaatmaja, *arXiv:1803*.04040

Elasto-Wetting

Jacco Snoeijer

University of Twente, the Netherlands

Droplets on highly deformable, elastic surfaces exhibit unusual wetting behaviour. The deformability of the substrate alters the contact angle with respect to Young's law, and we will contrast this case of "elasto-wetting" with that of electrowetting. In addition, the spreading dynamics on soft surfaces is fundamentally different from that on rigid surfaces, owing to viscoelastic effects.We report recent experimental and theoretical progress on the topic, and highlight some of the salient features of the solid's surface tension.

Driving Liquid Barrels with Electrowetting

Élfego Ruiz-Gutiérrez[1], Davood Baratian[2], Rodrigo Ledesma-Aguilar[1] and Frieder Mugele[2]
[1]*Smart Materials and Surfaces Laboratory, Northumbria University, Newcastle upon Tyne, NE1 8ST, United Kingdom*
[2]*Physics of Complex Fluids, MESA+ Institute for Nanotechnology, Department of Science & Technology, University of Twente, The Netherlands*

Liquid barrels—droplets trapped in a wedge geometry—appear in biological physics, granular media and microfluidics. Recent electrowetting experiments show that the equilibrium configuration of a liquid barrel is a truncated sphere that intersects the wedge walls with an equilibrium contact angle adjusted by the applied voltage [1] (see Fig. 1). The ability to control the motion of liquid barrels promises applications of droplet manipulation in microfluidic channels; however, the dynamics to new equilibria induced by sudden changes in voltage has not been studied in detail. In this talk, we present experiments and simulations of the dynamics of liquid barrels driven by electric fields.

The experimental setup (see Fig. 1) consists of two glass plates coated with indium tin oxide and fixed to form a wedge. The plates are treated with a layer of parylene-C using a chemical vapor polymerization process, and a thin layer of Teflon AF to form a dielectric hydrophobic coating [1]. Water droplets (KCl electrolitic solution; conductivity 5 mS cm^{-1}) were immersed in non-conducting bromohexadecane (of density 0.998 g cm^{-3} to avoid buoyancy effects), and driven by applying an alternating voltage.

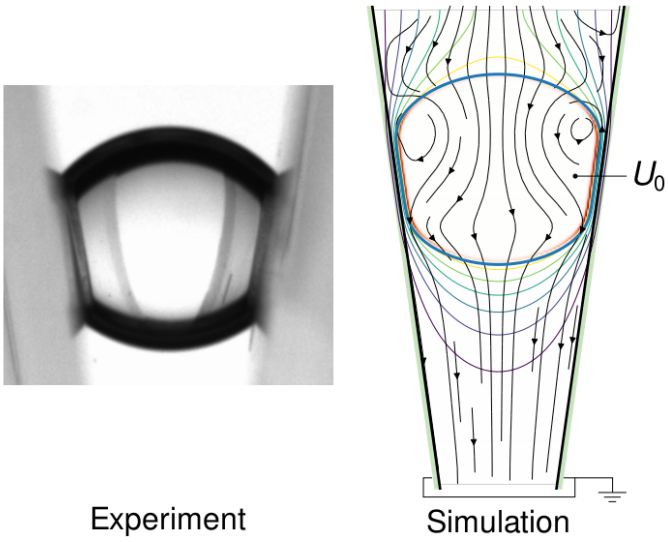

Figure 1. Experiments and simulations of a droplet moved by electrowetting.

To model the liquid-barrel dynamics, we carried out lattice-Boltzmann simulations of the coupled Navier-Stokes and Cahn-Hilliard equations [4] (see Figure 1). To account for electrowetting, we equipped our lattice-Boltzmann algorithm with a solver of the electric potential field; this allows us to analyse in detail the competition of viscous, capillary and electrostatic forces that act on the shape of the liquid-barrel.

From recent theoretical results [2], one might expect that the liquid barrel follows an exponential relaxation to equilibrium with a single characteristic time determined by the ratio of dissipative to restitutive forces. Surprisingly, we found that the dynamics occurs in two steps: a fast initial motion followed by a slow final relaxation. The dynamics of the first step is consistent with a relatively small dissipation [3], suggesting that a lubricating film allows the liquid barrel to slide without touching the wedge walls. This is different to the second step, in which the relaxation is paced by the motion of a contact line.

References

[1] D. Baratian, A. Cavalli, D. van den Ende, F. Mugele. *Soft Matter*, **11**, p. 7717-7721, (2015)

[2] É. Ruiz-Gutiérrez, C. Semprebon, G. McHale, R. Ledesma-Aguilar. *Journal of Fluid Mechanics*, **842**, p. 26-57, (2018)

[3] É. Ruiz-Gutiérrez, J.H. Guan, B. Xu, G. McHale, G.G. Wells, R. Ledesma-Aguilar. *Phys. Rev. Lett.*, **118**, p. 218003, (2017)

[4] T. Krüger, H. Kusumaatmaja, A. Kuzmin, O. Shardt, G. Silva, E.M. Viggen. *The Lattice-Boltzmann Method: Principles and Practice* Springer, 2016

Controlling the behavior of bubbles through dielectrowetting

A. M. J. Edwards[1], A. Roberts[1], M.I. Newton[1], I.C. Sage[1], G. McHale[2] and C.V. Brown[1]

[1]*School of Science and Technology, Nottingham Trent University, Clifton Lane, Nottingham NG11 8NS, UK.*
[2]*Smart Materials and Surfaces Laboratory, Department of Mathematics, Physics and Electrical Engineering, Northumbria University, Ellison Place, Newcastle upon Tyne NE1 8ST, UK.*
Presenting author: Carl Brown (carl.brown@ntu.ac.uk)

Trapped air bubbles attached to surfaces in liquids can be problematic in many applications. In microfluidics bubbles can block flow in channels and amplify the shear wall stress [1], and in pool boiling based heat exchanger devices bubbles can form dry patches, which dramatically reduce the heat flux coming from the surface which can lead to overheating and device failure [2]. Electrowetting on dielectric (EWOD) has previously been used to modify the wetting behavior of air bubbles, including demonstrating the ability to detach pinned bubbles [3]. Key issues in using EWOD in this context include the requirement for direct electrical contact with the liquid, plus a lack of subsequent control after the first actuation. We present a new method of controlling the wetting, the detachment, and moreover the subsequent surface adhesion behavior, of an air bubble in a liquid through dielectrowetting, an interface-localised form of liquid-dielectrophoresis [4]. This method allows bubbles to be removed on demand from the surface with the application of a critical detachment voltage to a patterned electrode on the surface. No electrical contact to the liquid itself is required, the method works regardless of the electrical conductivity of the liquid. Once detached, bubbles are free to float and can be prevented from re-attaching to the surface by a thin liquid layer that is maintained even when the applied voltage is reduced by around an order of magnitude compared to the critical detachment voltage. The figure shows how a liquid film is maintained between the bubble and the surface (inset). The thickness *h* of the film shows a logarithmic dependence on the magnitude of the voltage (main figure). We have developed a theory that provides an excellent description of how *h* , and the value of the critical re-attachment voltage at which *h* tends to zero, depends on the voltage, on the material parameters of the liquid, and on the geometrical parameters of the electrode pattern.

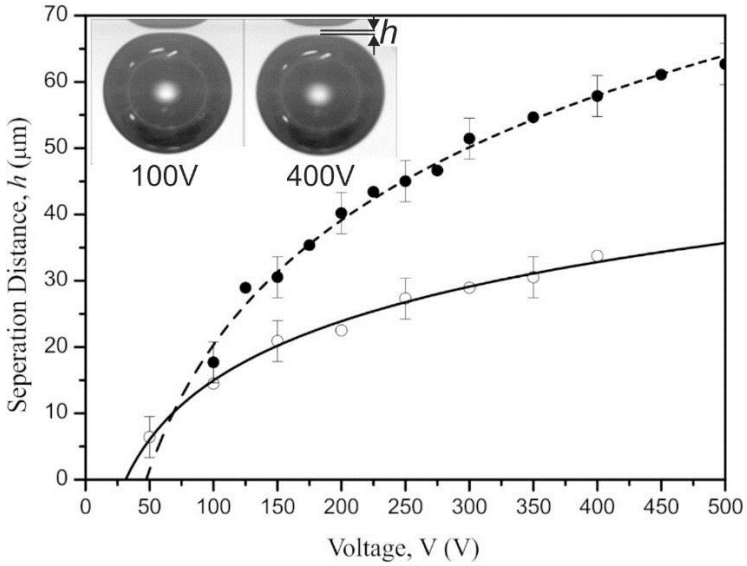

Figure: Voltage control of thickness *h* of the liquid film between a bubble and a solid surface for two different electrode patterns

References

[1] Cheng D and Jiang H, *Applied Physics Letters* **95**, 1 (2009)
[2] Raza MQ, Kumar N, Raj R, *Scientific Reports* **6**, 19113 (2016)
[3] Wang S, Chen HH, Chen CL, Wang S, Chen HH, Chen CL, *Applied Physics Letters* **108**, 181601 (2016)
[4] McHale G, Brown CV., Newton MI, Wells GG, Sampara N. *Physical Review Letters* **107**, 186101 (2011)

Mechanisms of wetting transitions of electrowetting on patterned surfaces: effect of surface topography, material wettability and dielectric thickness on reversibility

Nikolaos T. Chamakos[1], George Karapetsas[2] and Athanasios G. Papathanasiou[1]*
[1]*School of Chemical Engineering, National Technical University of Athens, 15780, Greece*
[2] *School of Chemical Engineering, Aristotle University of Thessaloniki, 54006, Greece*
**pathan@chemeng.ntua.gr*

When electrowetting is performed on a flat and smooth surface, fast and reversible apparent contact angle (ACA) modification is a trivial task. The reversibility however is lost for geometrically micro- patterned surfaces. Upon exceeding a threshold voltage, the liquid penetrates the surface pattern features and the well-known Cassie - Wenzel transition sets in. Then the outer liquid /solid / surrounding air three phase contact line (TPL) remains pinned, even if the voltage is removed; and this pinning appears even when surfaces with extreme hydro- or oleo-phobic properties are used [1].

Here we illuminate mechanisms of wetting transitions of electrowetting on patterned surfaces by means of realistic computational analysis (fig. 1)[2,3]. The equilibrium, as well as the dynamics of entire (mm-sized) droplets are computed by accounting for electric field distribution, coupled with moving interface profiles and liquid flow on micro-patterned surfaces. We investigate in detail the role of the various characteristics of the solid substrate (i.e the dielectric thickness, geometry and material wettability) on the spreading dynamics and the Cassie-Wenzel wetting transitions.

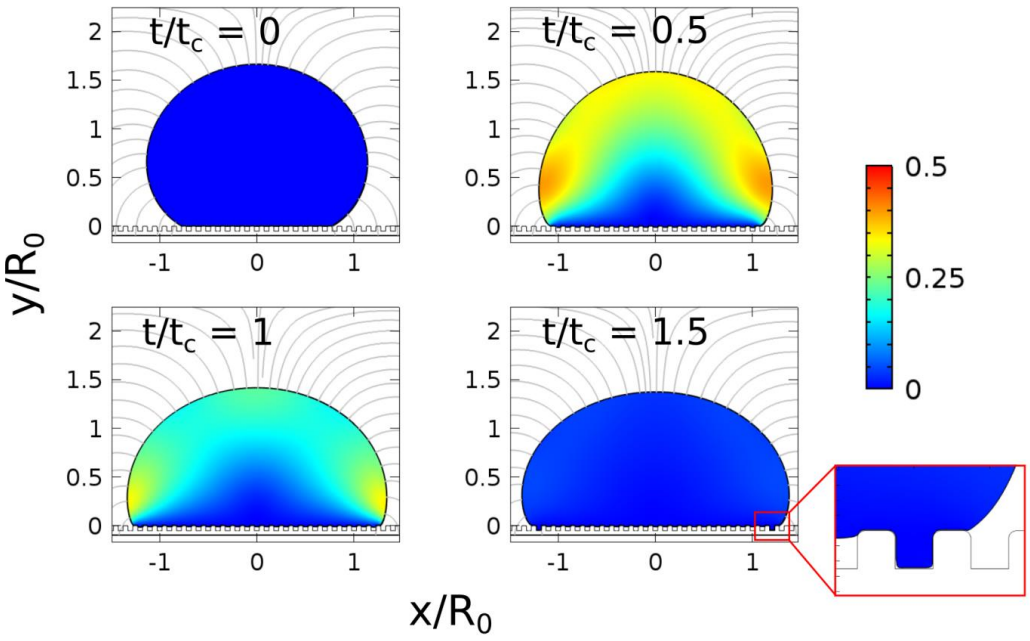

Fig.1. Spreading and partial penetration of a liquid drop on a patterned surface.

We reveal the critical role of the solid dielectric thickness on the electrowetting induced wetting transitions. By performing a multi-parameter solution space exploration we construct design maps for realizing reversibility on patterned surfaces. Such ability is of outmost importance for designing miniaturized devices (e.g. lab-on-a-chip) where the liquid-solid adhesion can be dynamically controlled.

References

[1]A. G. Papathanasiou, Current Opinion in Colloid & Interface Science, **36**, 70 (2018).
[2]N. T. Chamakos, M. E. Kavousanakis, and A. G. Papathanasiou, Langmuir, **30** (16), 4662 (2014).
[3]G. Karapetsas, N. T. Chamakos, and A. G. Papathanasiou, Journal of physics. Condensed matter, **28** (8), 085101 (2016).

Topic no. XX (see website/flyer)
Oral EW Conf. 2018

High-throughput electroactuation of droplets

Jean-Christophe Baret
Soft Micro Systems
Univ. Bordeaux, CNRS-UMR5031, Centre de Recherche Paul Pascal
115 Avenue Schweitzer - 33600 Pessac (France)

Droplet-based microfluidics is a key technology to perform biological assays at a ultra-high throughput. Over the past years, several platforms for droplet manipulations have been used to miniaturize assays and perform experiments that can not be done otherwise. The power of droplet-based microfluidics comes for the high level of parallelization achieved by manipulating emulsion droplets in microchannels. Yet, as millions of droplets can be manipulated in parallel, there is a need to specifically manipulate one or a few of specific droplets in large populations of drops, for example to select those droplets containing biological variants with extraordinary properties. Electric fields provide such a high level of control over emulsion droplets. Here we will describe and discuss the use of electric fields in droplet-based microfluidics and exemplify how electric fields provide key functions to perform highly controlled experiments at a ultra-high throughput for screening or for the bottom-up assembly of complex structures in miniaturized compartments

[1] Fluorescence-activated droplet sorting (FADS): efficient microfluidic cell sorting based on enzymatic activity, J.-C. Baret, et al. Lab Chip 9 1850 (2009)
[2] Microfluidic Flow-Focusing in ac Electric Fields, S. H. Tan, B. Semin and J.-C. Baret, Lab Chip, 14, 1099-1106 (2014)
[3] The Microfluidic Jukebox, S. H. Tan, F. Maes, B. Semin, J. Vrignon and J.-C. Baret, Scientific Reports 4, 4787 (2014)
[4] Sequential bottom-up assembly of mechanically stabilized synthetic cells by microfluidics, M. Weiss et al. Nature Materials, 17, 89-96 (2018)

Topic no. XX (see website/flyer)
Oral or poster EW Conf. 2018

On the Connection Between Droplet Velocity and Saturation in Digital Microfluidics

Ian Swyer[1], Ryan Fobel[1], and Aaron R. Wheeler[1]
[1]*Department of Chemistry, University of Toronto, 80 St George St., Toronto, ON, M5S 3H6, Canada*

In digital microfluidics (DMF) discrete droplets of fluid are actuated on top of an electrode array via electromechanical forces. Many authors to date have noticed that the dissipative forces on a droplet are linearly proportional to the droplet velocity, which often results in parabolic voltage-velocity plots [1,2]. There has been at least one report of contact angle saturation in the electrowetting on dielectric (EWOD) phenomenon, which was found to correspond to a velocity plateau in the voltage-velocity curve for water droplets moving in a one-plate DMF device [3]. Here we advocate for the use of force-velocity plots in lieu of voltage-velocity curves, provide a context for earlier observations of velocity saturation, **and demonstrate for the first time that force-velocity plots can be used to determine the force at which saturation phenomena such as those observed in electrowetted contact angles occur in two plate digital microfluidic devices.**

While complicated, the dissipative forces on a droplet actuated in DMF can be approximated as being linearly proportional to the droplet velocity. With this approximation, equation (1) shows that one should expect a plot of droplet velocity versus applied force should be linear.

$$ma = F_e - F_{threshold} - F_{contact} - F_{viscous} = F_e - F_{threshold} - (k_{contact} + k_{viscous})v$$

$$\therefore v = \left(1 - e^{-(k_{contact}+k_{viscous})\cdot t/m}\right)(F_e - F_{threshold})/(k_{contact} + k_{viscous}) \quad \textbf{(1)}$$

In equation 1, v is the velocity of the droplet, F_e is the applied force, F_{thres} is the threshold force that must be overcome to initiate droplet movement, $F_{contact}$ is the dissipative force associated with the contact line of the droplet, and $F_{viscous}$ is the viscous force on the droplet. From equation (1), if measurements of droplet velocity are made at a time $t \gg m/(k_{contact} + k_{viscous})$, then the velocity of the droplet should be directly proportional to the force applied. An interesting note is that if this linearity between droplet velocity and force were violated then it could indicate the presence of a non-linear dissipative mechanism, i.e. saturation.

Force-velocity plots for two surfactant solutions, one non-conductive and one conductive, moving back and forth between two 5.2 mm x 2.5 mm electrodes are shown in Figure 1. As expected from equation 1 the force-velocity curves are initially linear, but in non-conductive solutions (Fig. 1a), the velocity deviates from this linearity at around 27 mN/m. This deviation coincides with small droplets being ejected from the mother droplet and this droplet ejection becomes more vigorous as the force is increased (Fig. 1b). The force-velocity plot for the conductive solution (Fig. 1c) also shows deviation from linearity, but at a higher force and in the absence of droplet ejection. Noting that the addition of salt can suppress droplet ejection but lead to other saturation mechanisms such as air ionization [4] or charge injection [5] the passive (non-potentiated) aqueous contact angle on surfaces over these electrodes (in fresh droplets, after completing the actuation) was measured over time at forces around the saturation force (Fig. 1d). As shown, the contact angles decrease for surfaces that had been operated at or near the force-velocity saturation force, which is in line with expectations of charge injection or air ionization (no change was seen for 0.1 M NaCl controls).

These results cement the relationship between saturation phenomena seen in EWOD and DMF. We propose that force-velocity plots will be a useful tool to illuminate saturation characteristics and other device performance metrics for a wide range of applications.

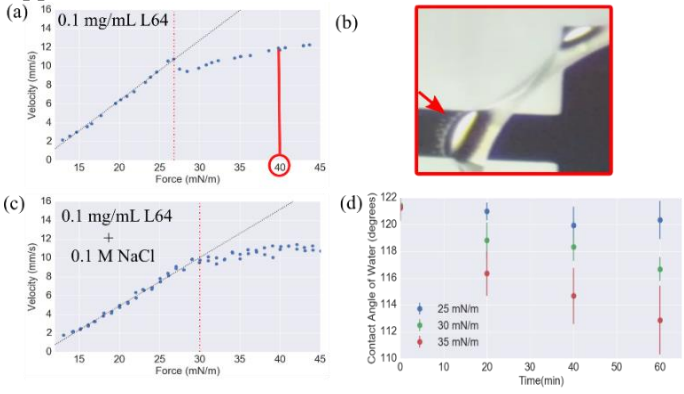

Figure 1: (a) Force velocity plot for 0.1 mg/mL L64 solution in DI water (b) Droplet ejection seen at around 40 mN/m for fore 0.1 mg/mL L64 solution (c) Force velocity plot fore 0.1 mg/mL L64 + 0.1 M NaCl solution (d) Contact angle of electrodes running 0.1 mg/mL L64 + 0.1 M NaCl solution droplet back and forth at 25, 30, and 35 mN/m. Contact angle decreases starting at the saturation force 30 mN/m.

[1] V. Jain, A. Hole, R. Deshmukh and R. Patrikar, Sensors and Actuators A: Physical, 224–233, (2017).
[2] J. H. Song, R. Evans, Y.-Y. Lin, B.-N. Hsu and R. B. Fair, Microfluid Nanofluid, 75–89, (2009).
[3] H. Ren, R. B. Fair, M. G. Pollack and E. J. Shaughnessy, Sensors and Actuators B, 201–206, (2002).
[4] M. Vallet, M. Vallade and B. Berge, Eur. Phys. J. B, **11**, 583–591, (1999).
[5] A. I. Drygiannakis, A. G. Papathanasiou and A. G. Boudouvis, Langmuir, **25**, 147–152, (2009).

Topic no. 1, 6, 7
Oral
EW Conf. 2018

Anti-Biofouling by Integrating SLIPS (Slippery Liquid Infused Porous Surface) with Electrowetting and Liquid Dielectrophoresis (L-DEP)

Hong Yao Geng and Sung Kwon Cho
University of Pittsburgh

Biofouling or molecule adsorption to surfaces is one of the critical problems in many lab-on-a-chip systems. In particular, this is even more detrimental to digital microfluidics based on electrowetting or dielectrowetting (liquid dielectrophoresis) in which indispensable hydrophobic surfaces are in direct contact with working bio-solutions. Up to date, there have been attempts to mitigate this critical problem: e.g., using oil for the filler fluid, adding additives to bio-solutions, treating the hydrophobic surfaces, etc. However, these methods still have their own drawbacks. In this talk, we present the integration of a SLIPS (slippery liquid infused porous surface) with electrowetting and liquid dielectrophoresis (L-DEP). This configuration is experimentally confirmed highly effective for efficiently minimizing biofouling in electrowetting as well as L-DEP droplet manipulations.

The SLIPS [1] consists of a porous layer infused with lubricating oil such that working fluids in the microfluidic chip virtually have a liquid-to-liquid contact, not direct solid contact, when the SLIPS covers the microfluidic chip surface. The SLIPS enormously reduces biomolecule adhesion because of the highly mobile and deformable nature of liquid. That is, biomolecules can move easily on the SLIPS. Previously, there have been attempts to integrate a SLIPS with electrowetting [2] and dielectrowetting [3]. However, their studies have been limited to dynamics and contact angle hysteresis with pure liquid sessile droplets. Effects of the SLIPS on biofouling in digital microfluidics have never been studied. In the present study, the biofouling effects are examined for sessile droplets as well as laterally transporting droplets by electrowetting as well as L-DEP integrated with the SLIPS.

To integrate the SLIPS, a porous ePTFE thin film (thickness: 8 μm, pore size: 200-500 nm) infused with Krytox-103 lubricating oil covers the top of the conventional dielectric layer (2-μm thick SU-8 layer) in electrowetting and L-DEP. Underneath the dielectric layer, the arrayed coplanar electrodes were patterned to a solid shape for electrowetting as well as L-DEP. As testing fluids, water, protein (fluorescent bovine serum albumin or BSA, 1 mg/ml), sheep blood and whole milk droplets for electrowetting and propylene carbonate and isopropyl alcohol (IPA) droplets for L-DEP were selected and examined, respectively.

First of all, it is experimentally confirmed that all droplets of the above six fluids are smoothly and repeatedly transported from one electrode to next by elelctrowetting or L-DEP, although there exist differences in transporting speeds. Next, bio-fouling is extensively examined using the BSA droplets. BSA droplets were placed on a regular hydrophobic Teflon, ePTFE (no lubricating oil) and SLIP surfaces, respectively, and exposed to the atmospheric condition for a while to evaporate them. After complete evaporation, BSA molecules are widely deposited on the Teflon and ePTFE surfaces (often forming coffee ring patterns), while they form into a single dot on the SLIPS (Fig. 1, most left photos). This is because the molecules on the SLIPS are mobile so they move laterally as the droplet evaporates and thus the three-phase contact line recedes. During the evaporation process, the contact angle of the BSA droplet on the SLIPS maintains at the initial contact angle (~110°) without decreasing. However, with the BSA droplets on the Teflon and ePTFE surface, the contact angles significantly decrease. Finally, the BSA deposits were attempted to clean using electrowetting-actuated fresh water droplets as shown in Fig. 1. A fresh droplet covers the BSA dried area for a while to dissolve the deposited BSA molecules and then is attempted to transported to the left by electrowetting. On the Teflon surface, the droplet cannot move (third photo in Fig. 1(a)), while on the SLIPS the droplet can easily move to the left (Fig.1(b), third photo) since most of the deposited molecules are captured from the SLIPS. Anti-biofouling with the SLIPS was also confirmed by the fluorescent images showing bio-fouled proteins (green) on the regular Teflon electrowetting chip but no bio-fouled proteins noticed on the SLIPS electrowetting chip (no green) (most right in Fig.1 (a), (b)). More detailed measurements and discussions will be presented in the talk.

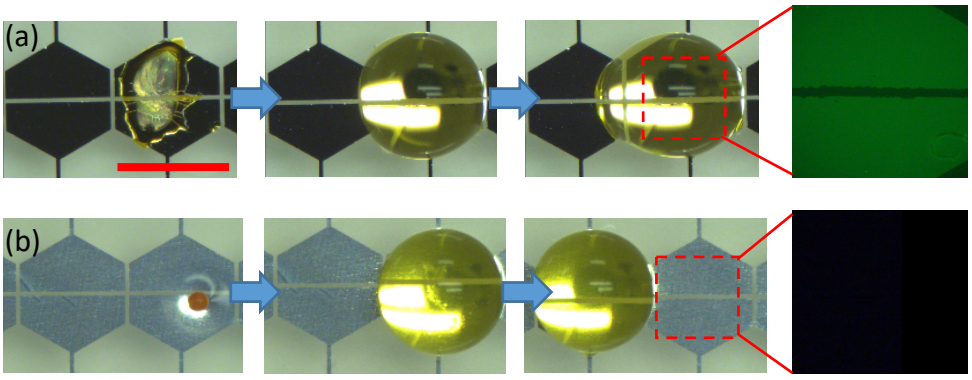

Figure 1 (a) Electrowetting with a Teflon surface without SLIPS fails to move a BSA droplet due to bio-fouling.
(b) Electrowetting with SLIPS resume to easily move a BSA droplet (anti-biofouling). The green in the fluorescent images (most right) indicate the presence of bio-fouled BSA residues on the surface. The scale bar is 1.5 mm.

References:
[1] T.-S. Wong *et. al.*, *Nature*, Vol. 477, pp. 443-447 (2011).; [2] C. Hao *et. al.*, *Scientific Reports*, Vol. 4, p. 6846 (2014).; [3] Z. Brabcova, *et. al.*, *Applied Physics Letters*, Vol. 110, p. 121603 (2017).

Reconfigurable Ion Selective Sensor Array Enabled by Digital Microfluidics

Ali Farzbod and Hyejin Moon
Mechanical and Aerospace Engineering Department, University of Texas at Arlington
Arlington, TX 76019, USA

This paper presents a demonstration of a reconfigurable ion selective electrodes (ISE) array enabled by an electrowetting on dielectric (EWOD) digital microfluidics, for the first time. The on-chip fabrication of an ISE array includes electroplating Ag followed by forming AgCl layer by chemical oxidation, and forming a thin layer of arbitrary ion-selective membrane liquid on a sensor electrode. Although ISEs are widely used, fabrication and implementation of typical ISE to miniaturized systems are limited because they are generally bulky to meet the requirements of supporting matrix and plasticizer to hold liquid membrane stably. Some solid-state sensors can work as ISE [1], but they do not take advantages of liquid membranes and has limited capability. Recently, a paper-based ISE has been developed [2] but there are issues such as drift in calibration curve and lack of ability to change the selective membrane. Moreover, the lifetime of a typical ISE is limited due to dissolving of AgCl layer [3]. To tackle these problems, we utilized the liquid handling capability of digital microfluidics to build a reconfigurable ISE.

Demonstration includes; 1) dispense and delivery of nanoliter volume droplets of Ag electroplating solution to sensor electrodes, 2) on-chip electroplating and chemical oxidation to obtain Ag/AgCl reference and working electrodes, 3) forming thin-film of ion-selective membrane solutions by using EWOD microfluidic motion, 4) ion selective sensor performance by Nerstian responses, and 5) dissolving liquid membrane and washing sensor electrode followed by reconfiguration and renewal of degraded sensors. This successful demonstration promises that the proposed reconfigurable ISE can provide a sensor device where a user can define and form desirable ISEs instantaneously at the time of use. Simultaneous (and/or serial) detection of multiple analytes will be available.

[1] M. Piao, J. Yoon, Y. Shim, and S. Korea, "Characterization of All Solid State Hydrogen Ion Selective Electrode Based on PVC-SR Hybrid Membranes," *Sensors*, vol. 3, pp. 192–201, 2003.

[2] M. Novell, M. Parrilla, G. a. Crespo, F. X. Rius, and F. J. Andrade, "Paper-based ion-selective potentiometric sensors," *Anal. Chem.*, vol. 84, pp. 4695–4702, 2012.

[3] B. J. Polk, A. Stelzenmuller, G. Mijares, W. MacCrehan, and M. Gaitan, "Ag/AgCl microelectrodes with improved stability for microfluidics," *Sensors Actuators B Chem.*, vol. 114, no. 1, pp. 239–247, Mar. 2006.

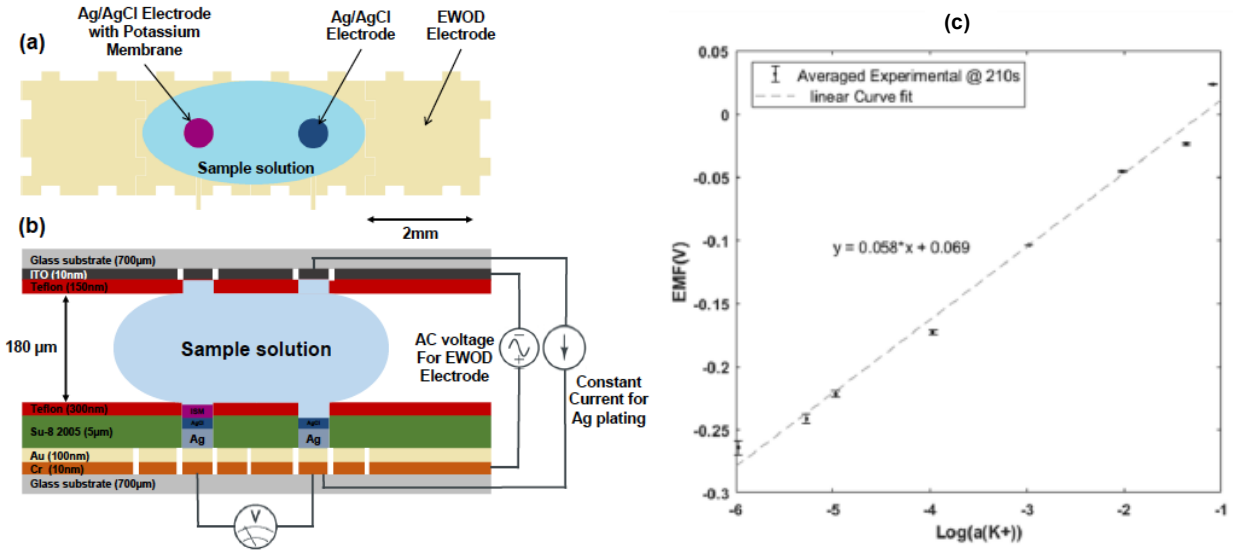

Figure. **(a)** The top view of the schematics of an electrochemical cell integrated with EWOD electrodes, **(b)** The side view of the electrochemical cell with the electrical circuits for EWOD DMF operation, electroplating and potentiometric measurements, and **(c)** The Nernstian response to the different molarity of KCl solutions (e.g. sensor calibration curve).

New Electrowetting Phenomena Using Liquid Metal

Collin Eaker[1], Ishan D. Joshipura[1], Rashed Khan[1], David Hight[1], John O'Reagan[1],
Jason Heikenfeld[2], Karen Daniels[3], and Michael D. Dickey[1]
[1]NC State, Chemical and Biomolecular Engineering
[2]University of Cincinnati, Electrical Engineering, [3]NC State, Physics

This talk will discuss the use of gallium-based alloys for various electrowetting phenomena. These alloys, which have both metallic and liquid properties, are notable because they have low toxicity, zero vapor pressure, and react with air to form a native oxide 'skin'. We have studied this material for electrowetting in three ways:

1. Liquid metal can simply be 'painted' on a substrate (i.e. no vacuum processing) to create soft, stretchable electrodes for electrowetting-on-dielectric (EWOD), as shown in Fig. 1a-c. The native oxide, which is ~3 nm thick, serves as a self-healing dielectric while maintaining the liquid in the shape of a flat electrode[1]. EWOD occurs without external voltage via short circuiting due to the built in open circuit potential (Fig. 1, d-e)[2].
2. Normally the native oxide adheres to the walls of capillaries and limits the ability of the metal to flow. Prefilling capillaries with water creates a 'slip layer' between the oxide-coated metal and the capillary walls. This slip layer enables continuous electrowetting of a plug of liquid metal as a means of translating it back and forth[3].
3. Perhaps most surprising, electrochemical oxidation of gallium alloys significantly lowers the interfacial tension using 1 V[4]. At this potential, the metal spreads into fractal shapes (Fig 1. f), suggesting the interfacial tension approaches zero[5]. Reversing the potential removes the native oxide and returns the metal back to a state of high tension[6]. Thus, it is possible to rapidly and reversibly modulate the tension by ~500 mN/m using only 1 V.

Taken in sum, these techniques represent simple and effective ways to move and manipulate liquid metals for reconfigurable electronics, optics, and switches[7].

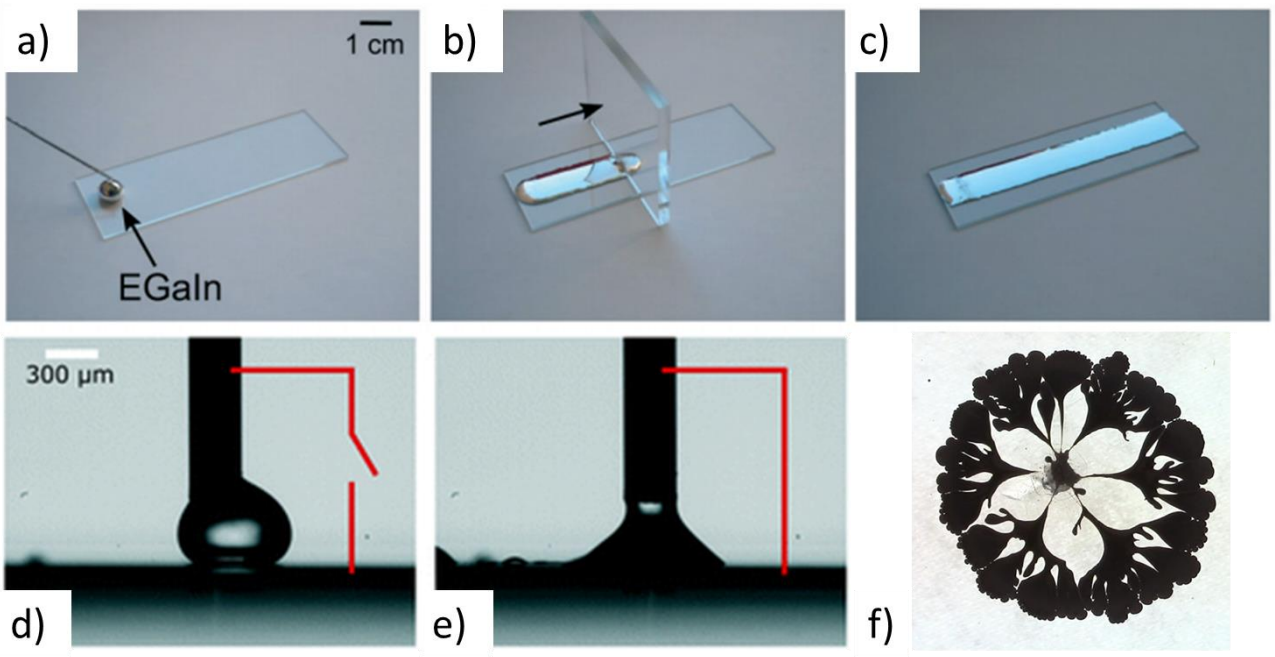

Figure 1. (a-c) "Paint-on" EWOD electrodes composted of eutectic gallium indium (EGaIn). (d-e) EWOD of a droplet of water without external potential achieved via short circuiting the needle and liquid metal substrate. (f) Liquid metal forms fractals at 1 V due to oxidation.

References

[1] C. B. Eaker, I. D. Joshipura, L. R. Maxwell, J. Heikenfeld, M. D. Dickey, *Lab. Chip* **2017**, *17*, 1069.
[2] M. D. Dickey, *Adv. Mater*. **2017**, 1606425.
[3] M. R. Khan, C. Trlica, J.-H. So, M. Valeri, M. D. Dickey, *ACS Appl. Mater. Interfaces* **2014**, *6*, 22467.
[4] M. R. Khan, C. B. Eaker, E. F. Bowden, M. D. Dickey, *Proc. Natl. Acad. Sci.* **2014**, *111*, 14047.
[5] C. B. Eaker, D. C. Hight, J. D. O'Regan, M. D. Dickey, K. E. Daniels, *Phys. Rev. Lett.* **2017**, *119*, 174502.
[6] M. R. Khan, C. Trlica, M. D. Dickey, *Adv. Funct. Mater.* **2015**, *25*, 671.
[7] C. B. Eaker, M. D. Dickey, *Appl. Phys. Rev.* **2016**, *3*, 031103.

Dynamics of ultra-low voltage electrowetting using graphite surfaces

P. Kant[1], B. Etcheverry[2], P. Iamprasertkun[3], H.V. Patten[3], R.A.W. Dryfe[3] & A. Juel[1]

[1]*MCND, School of Physic & Astronomy, University of Manchester, Manchester, UK*

[2]*Ecole Normale Supérieure de Lyon, Lyon, France*

[3]*School of Chemistry, University of Manchester, Manchester, UK*

Electrowetting is a powerful method to achieve external wetting control, by exploiting the potential-dependence of the liquid contact angle with respect to a solid substrate. Addition of a dielectric film to the surface of the substrate, which insulates the electrode from the liquid thereby suppressing electrolysis, has led to technological advances such as variable focal-length liquid lenses, electronic paper and the actuation of droplets in lab-on-a-chip devices. The presence of the dielectric, however, necessitates the use of large bias voltages (frequently in the 10–100 V d.c. range). Here we focus on a simple, dielectric-free approach to electrowetting using the basal plane of graphite as the conducting substrate [1]. We find unprecedented changes in contact angle for ultra-low voltages below the electrolysis threshold, which are reproducible, stable over 100 s of cycles and free of hysteresis.

We vary the concentration of electrolyte in the drop by three orders of magnitude (10^{-3}M to 1M KF in water) and find a reduction of the electrowetting effect for negative applied potentials, whereas for positive applied potentials the variation of the wetting angle of the drop with applied potential is independent of the electrolyte concentration within the studied range.

We exploit the fact that the contact angle remains constant with variations in concentration (for positive applied potentials) to investigate the influence of electrolyte concentration on the dynamics of spreading. We find that the characteristic time of spreading increases linearly with the reduction of the electrolyte concentration of the drop while the drop radius versus time curve remains similar (Figure 1). We show that the hydrodynamic spreading time scale is limited by the electrokinetic time scale required to form an electrical double layer at the surface of the substrate, which in turn controls wetting through its capacitance.

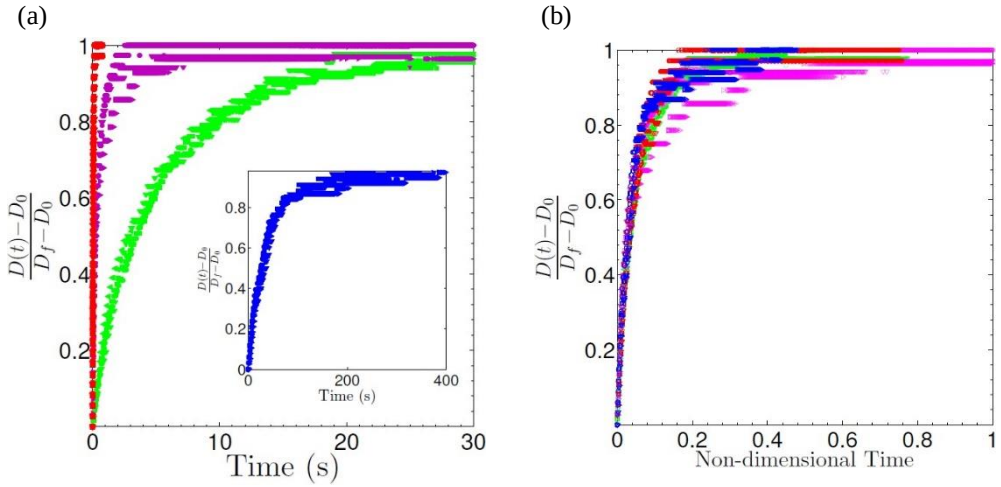

Figure 1: Dimensionless droplet diameter as a function of time for different KF concentrations in water: 1M (red), 0.1M (magenta), 0.01M (green), 0.001M (blue). The rate of spreading decreases with decreasing concentration. (a) dimensional time, (b) rescaled time: the characteristic rescaling time varies linearly with concentration.

[1] D.J. Lomax, P. Kant, A.T. Williams, H.V. Patten, Y. Zou, A. Juel and R.A.W. Dryfe 2016 Ultra-low voltage electrowetting using graphite surfaces Soft Matter 12, 8798 (2016).

Voltage dependent transition of interfacial capacitances on graphite surfaces

Jitesh Barman, Shao Wan, Tang Biao*, Jan Groenewold and Guofu Zhou
Electronic Paper Display Institute, South China Normal University, Higher Education Mega Center, Guangzhou, China - 510006

Electric field induced wettability modulation of a conducting drop via electrowetting has been used extensively in plethora of real life applications *e.g.* Lab - on - a - chip device, liquid lens, electronic displays etc. The wettability of the drop is mainly manipulated using the electrowetting on dielectric (EWOD) configuration by charging or discharging of a dielectric insulator between the conducting substrate and the drop. The advantage of introducing a thin insulator is to protect the system from electrolysis and other electrochemical events. However, the insulator costs a large bias voltage of the order of tens to hundreds of Volts to induce a significant contact angle change, which brings dielectric failure risk and hinders the low-power portable applications. Recently, reversible low voltage electrowetting phenomena on conductive highly-oriented-pyrolytic-graphite (HOPG) surfaces based on the charging of electrical double layers (EDL)[1] and pseudo-capacitor (PC) due to intercalation (IC) and de-intercalation (DIC) of ions[2] are demonstrated. In this presentation, bias voltage dependent transition of the interfacial capacitance between EDL and PC on HOPG surfaces for low voltage electrowetting will be discussed.

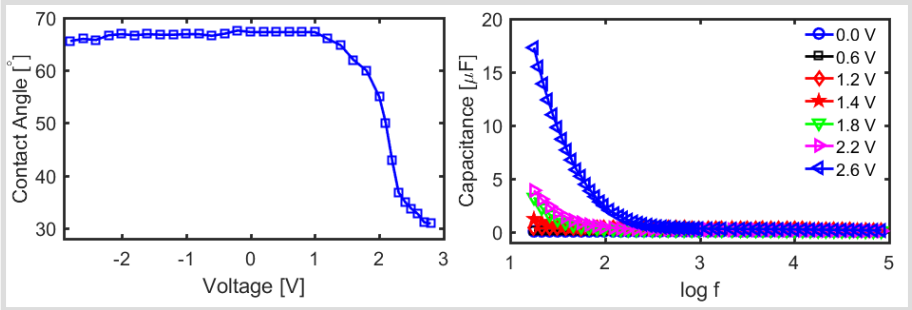

Fig. 1: (a) Apparent contact angle of a conducting droplet as a function of voltage on Highly-oriented-pyrolytic-graphite (HOPG). (b) Solid-liquid interfacial capacitance as a function of frequency for different applied bias voltage.

Fig. 1 (a) shows the apparent contact angle at 0 V of a 5 μL drop of 3 M LiCl aqueous solution on a freshly cleaved HOPG surface which is around 64 º. The contact angle doesn't change upon application of negative voltage on the substrate as well as low positive voltage upto 1.2 V, however, beyond that voltage the apparent contact angle decreases rapidly to a value around 30 º at 2.8 V. This sharp decrease in contact angle of the drop is due to the transition in capacitor formation at the liquid-solid interface; below 1.2 V, EDL based capacitor is formed whereas above 1.2 V, IC-DIC based PC plays the significant role to change the contact angle. The appearance of reduction peak at 0.4 Vin the positive CV scans for voltages greater than 1.2 V confirms the intercalation of Cl^- ions into the graphene layers. Fig. 1 (b) shows the measured capacitance of the solid-liquid interface as a function of frequency for different applied voltages measured by EIS technique. The capacitance remains constant for the whole range of frequency for voltages lower than 1.2 V, whereas, above 1.2 V the capacitance increases rapidly for the low frequency range. This quantitative study on the electrowetting and transition of interfacial capacitance on graphite would provide a deeper understanding to the electrowetting community on the ultra low voltage electro-capillary phenomenon on conductors for real life applications.

References:

1. D. J. Lomax, P. Kant, A. T. Williams, H. V. Patten, Y. Zou, A. Juel, and R. A. W. Dryfe, Soft Matter, 12, 8798-8804 (2016).
2. G. Zhang, M. Walker, and P. R. Unwin, Langmuir, 32, 7476 - 7484 (2016).

Oscillating Dynamics of a Protean Liquid Meniscus

Sri Ganesh Subramanian, Shikha Saluja, and Sunando DasGupta

Indian Institute of Technology Kharagpur, India – 721302

In this study, we report the captivating dynamics of an extended meniscus atop a silicon substrate, when it is subjected to multiple waveforms (viz. positive ramp, negative ramp, and sinusoidal) of alternating voltages, at different frequencies. We observed that the application of a time-varying voltage to an extended meniscus, resulted in several intriguing dynamics which are markedly different from that of droplets. [1] We descry that the liquid meniscus oscillates in both forward and backward directions, in accordance with the nature of the driving force, thereby resulting in a sequential wetting and dewetting phenomena. We applied the principles of interferometry to precisely calculate the film-thickness, which in turn, was used to determine the curvature and slope of the extended meniscus (see Figure 1 (a)). Furthermore, the film-displacement was also calculated, and the instantaneous velocity and acceleration were obtained for different voltage-frequency combinations, as a function of various waveforms (see Figure 1 (b)), using a MATLAB (R 2015b) subroutine. The nature of the instantaneous acceleration (see Figure 1 (b)), clearly demonstrates the fact that the film responds in accordance with the driving force, thereby substantiating the versatility of the extended meniscus. We also observed that the nature of the forcing function plays a crucial role in modulating the dynamics of the liquid meniscus, as evidenced from the curvature plot (see Figure 1(a)), wherein we discern a significant variation in the curvature due to the net effect of the forcing functions. We postulate that the dynamics of the film displacement could be successfully explained by considering the product of the applied electric field and its gradient, as opposed to the existing consideration of a square dependence on the applied field. [2] We conjecture that the ability to translate an extended meniscus in any possible manner (depending on the nature of the driving force), and in both the directions (forward and backward), would pave the path towards the development of novel microfluidic systems.

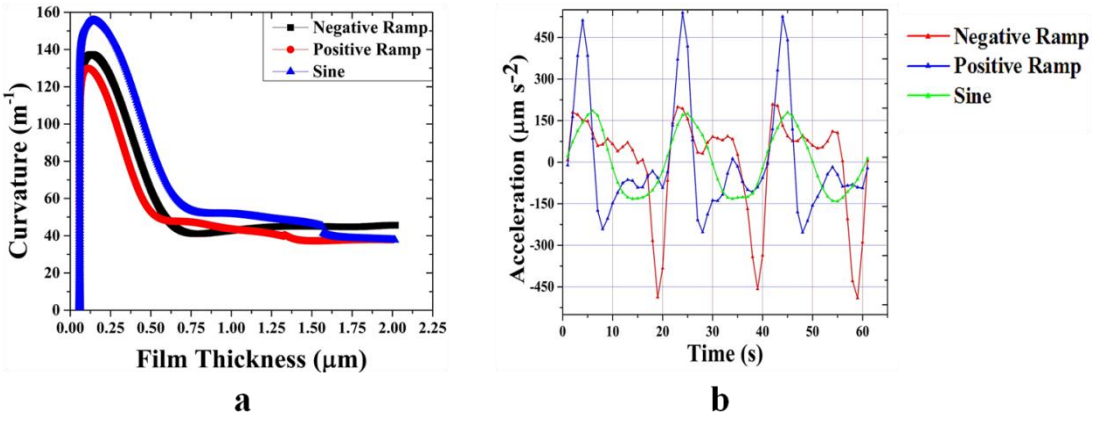

Figure 1 (a): Variation in the curvature of the liquid meniscus, as a function of film-thickness, for various waveforms, at 2 Vpp and 500 mHz. **1(b):** Temporal variation in the instantaneous acceleration of the liquid film, for different waveforms, at 2 Vpp and 1 Hz.

References:

[1] J. M. Oh, S. H. Ko, and K. H. Kang, Langmuir **24**, 8379 (2008).

[2] F. Li and F. Mugele, Appl. Phys. Lett. **92**, 1 (2008).

Topic no. XX (see website/flyer)
Oral or poster EW Conf. 2018

3D Heterogeneous Architectures Formation on an Electromicrofluidic Platform

Shih-Kang Fan
Department of Mechanical Engineering, National Taiwan University

Manufacturing three-dimensional (3D) architectures through assembly of prepolymer hydrogel droplets with suspended cells/particles/molecules and crosslinked building blocks with reorganized embedded objects is demonstrated on an electromicrofluidic platform. The complex and heterogeneous 3D architectures are in great demand in various applications, including in the production of novel metamaterials with properties atypical or nonexistent in nature or in the construction of artificial tissues that recapitulate physiological functions by imitating biological structures. 3D hydrogel building blocks with reorganized cells or particles are formed and assembled on the electromicrofluidic platform adopting electrowetting and dielectrophoresis [1, 2]. We demonstrate the manipulations of varied objects (a) in multiple phases such as prepolymer liquid hydrogel droplets (PEGDA, poly(ethylene glycol) diacrylate or GelMA, gelatin methacryloyl) and crosslinked hydrogel building blocks, (b) on a wide range of scales from micrometer cells or particles to millimeter assembled hydrogel architectures, (c) with diverse properties such as conductive and dielectric prepolymer droplets that are photo, chemically, or thermally crosslinkable, and (d) in adjustable geometries including discrete droplets and continuous liquid columns. 3D hydrogel architectures, composed of varied particles or cells reorganized in programmable patterns and biomimetic hydrogels of designed properties and in adjustable geometries, are obtained. The electromicrofluidic platform is general and alternative to manipulate particles/cells and prepolymer solutions for reconfigurable 3D architectures.

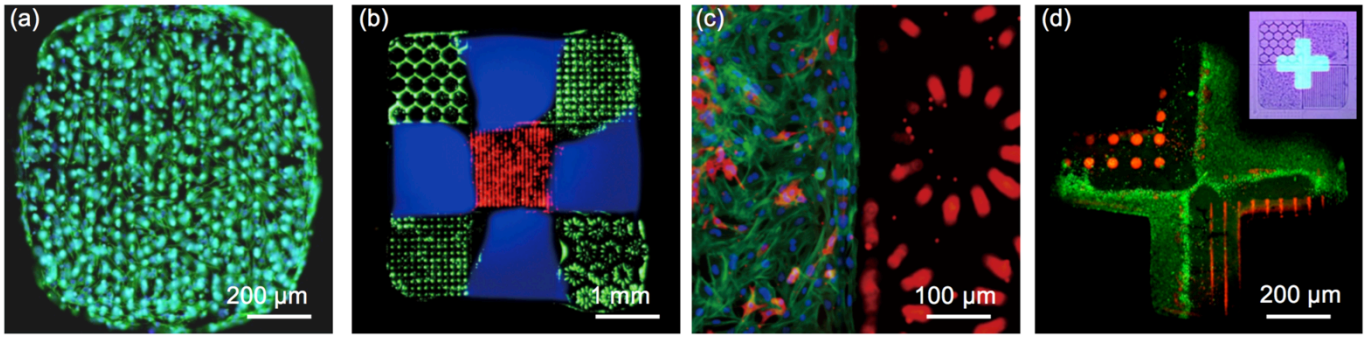

Figure 1 Constructing 3D building blocks and architectures on an electromicrofluidic platform. (a) A building block made of a GelMA hydrogel droplet and reorganized NIH 3T3 fibroblasts [1]. (b) An architecture with 3x3 assembled PEGDA droplets with fluorescent dye and particles [1]. (c) Neonatal mouse cardiomyocytes patterned on the surface of a hydrogenous architecture consisting GelMA and PEGDA [1]. (d) A PEGDA building block crosslinked by patterned light.

Reference:

[1] M.-Y. Chiang, Y.-W. Hsu, H.-Y. Hsieh, S.-Y. Chen, S.-K. Fan, Science Advances, **2**, e1600964 (2016).
[2] S. Takeuchi, Nature, **541**, 470-471 (2017).

Topic no. XX (see website/flyer)
Oral or poster EW Conf. 2018

Patterning thin liquid layers by electrode-free pyro-electrowetting

S. Grilli, R. Rega, L. Miccio, V. Vespini, V. Pagliarulo, A. Bramanti and Pietro Ferraro
Institute of Applied Sciences and Intelligent Systems of the National Research Council (CNR-ISASI)
Via Campi Flegrei 34, 80078 Pozzuoli (NA), Italy

The ability to pattern the arrangement of thin liquid layers is of crucial importance for a wide variety of applications including patterning nanoparticles dispersed into liquid phases [1], liquid actuation in integrated microfluidics [2,3] or in biology for drug and gene delivery [4,5]. Different techniques have been proposed in literature for these purposes and electrowetting is one of the most widely used. Appropriate electrodes and external circuits enable the application of local voltage profiles, which, in turn, are able to modulate the wetting properties of a surface by means of free electrical charges [6,7]. Here we present an innovative electrowetting process obtained by the pyroelectric effect induced into periodically poled ferroelectric crystals (e.g. lithium niobate). The crystal is spin-coated by a thin layer of liquid (mineral oil or PDMS) and subjected to an appropriate thermal stimulation by a conventional hot plate. The pyroelectric effect occurring into the crystal generates an array of surface uncompensated charges with opposite sign according to the reversed domain pattern, leading to a selective electrowetting. We show here the possibility of producing arrays of liquid microlenses [8] as well as arrays of micro-bumps made of cross-linked PDMS [9]. The method extends the applicability of electrowetting to all of those applications where the electrode and circuit fabrication represent an open issue.

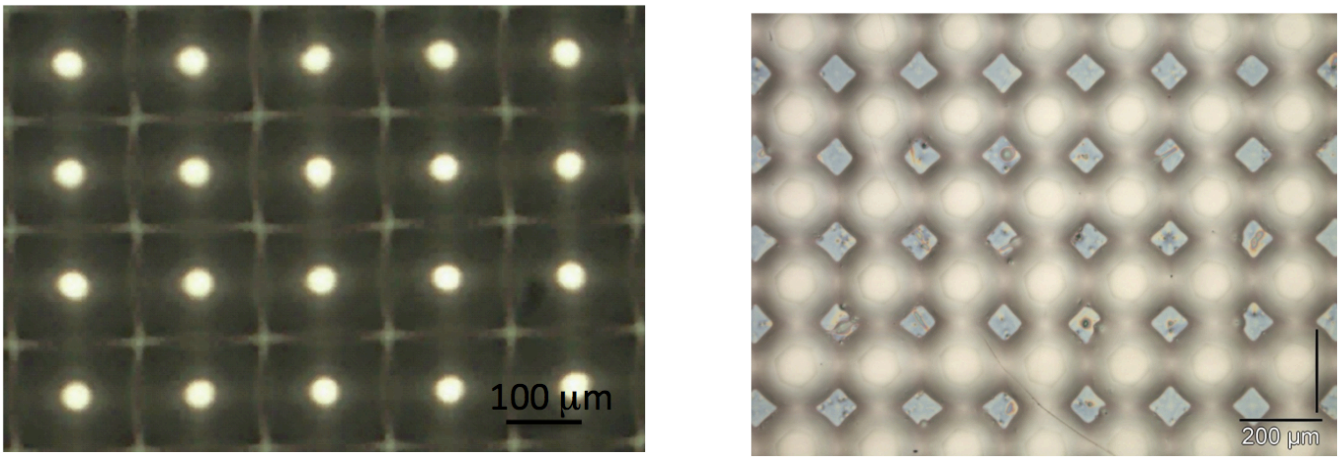

(a) (b)

Figure 1. Optical microscope images of a square array of (a) focusing liquid microlenses and of (b) soft solid-like micro-bumps made of cross-linked PDMS.

References:

[1] S. Liu et al., Small 21448 (2006).
[2] C.U. Murade e al. Optics Express 20, 18180 (2012).
[3] D. Psaltis et al. Nature 442, 381 (2000).
[4] I.A. Aksay et al. Science 273, 892 (1996).
[5] M. Mrksich et al. Annu. Rev. Biophys. Biomol. Struct. 25, 55 (1996).
[6] F. Mugele et al. J. Phys.: Condens. Matter 17, R705 (2005).
[7] J. Zeng et al. Lab on Chip 4, 265 (2004).
[8] S. Grilli et al. Optics Express 16, 8084 (2008).
[9] S. Grilli et al. Langmuir 24, 13262 (2008).

Breath figures under electrowetting

Ranabir Dey, Davood Baratian, Harmen Hoek, Dirk van den Ende, Frieder Mugele
Physics of Complex Fluids, MESA+ Institute for Nanotechnology, University of Twente, PO Box 217, 7500 AE Enschede, The Netherlands

We show that an electric field in an electrowetting (EW) configuration (Fig. 1(a)) can be used to actively control the pattern of drops condensing onto flat hydrophobic surfaces (breath figures). Understanding condensation of vapor on functionalized surfaces is scientifically challenging and simultaneously technologically relevant (heat transfer; fog harvesting). A quantitative description of the positional and size distribution of the drops, in conjunction with electrostatic energy calculations, reveals how EW strikingly modifies condensation patterns by aligning drops and enhancing coalescence (Fig. 1(b)). Such alignment results in a definite periodicity of the droplet pattern, which is determined by the electrode geometry. The EW-controlled evolution of drop condensation pattern significantly alters the statistical characteristics of the entire ensemble of droplets from those established for classical breath figures. A scaling analysis shows that under EW, the evolution of the drop size distribution displays self-similar characteristics that significantly deviate from classical breath figures on homogeneous surfaces once the electrically induced coalescence cascades set in beyond a certain critical drop size. We also show using preliminary heat transfer measurements that the droplet pattern characteristics under EW eventually lead to enhanced net heat transfer. We hope that this study will not only trigger a general theoretical analysis of drop condensation patterns in arbitrary energy landscapes but will be also useful for optimizing various applications involving dropwise condensation, like heat exchangers.

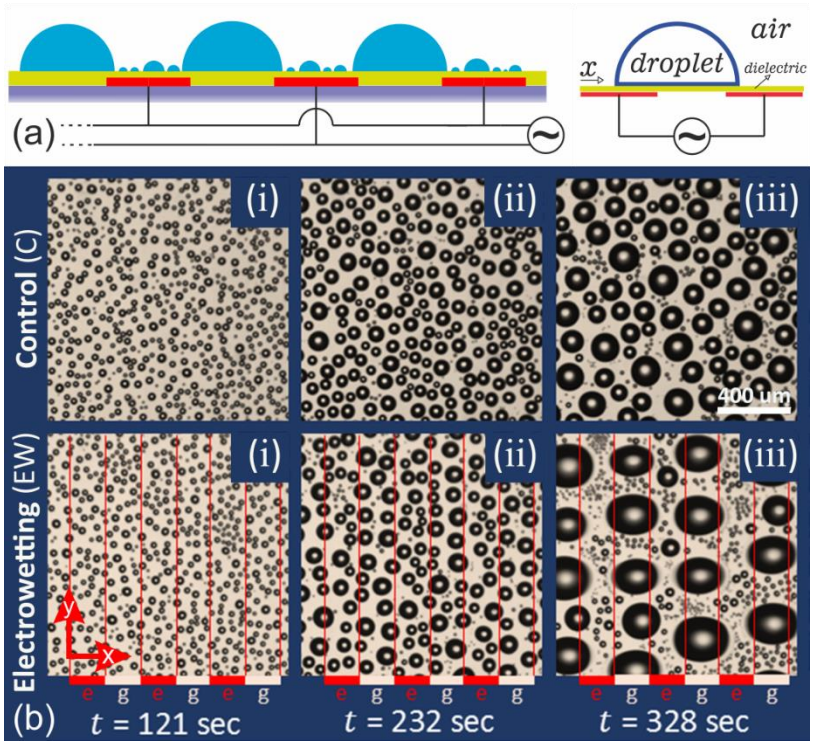

Fig 1(a) Schematic of the substrate used for the condensation experiments. Transparent interdigitated ITO electrodes are patterned on the glass substrate, which is then coated with a hydrophobic dielectric polymer film. A schematic of a condensate droplet under EW is also shown. (b) Comparison between breath figures without EW (control) (C-i to C-iii) and under EW (U_{rms} =150 V; f=1 kHz) (EW-i to EW-iii) at different time (t) instants. The (e)lectrode-(g)ap geometry underneath the dielectric film is indicated by the solid red and white lines. Gravity points from top-to-bottom i.e. along the negative y--direction.

REF:

(1) Physical Review Letters 120 (21), 214502, 2018.

Topic no. 8 (Novel applications)
Oral EW Conf. 2018

Electrowettability-based control & enhancement of phase change phenomena: New concepts and applications

Arjang Shahriari[1], Onur Ozkan[1], Enakshi Wikramanayake[1], Palash Acharya[1], ***Vaibhav Bahadur (VB)** [1]
[1] *Department of Mechanical Engineering, The University of Texas at Austin, Austin, USA*

Phase change phenomena (boiling, condensation, freezing) affect the performance and efficiency of numerous engineering systems. Liquid-solid wettability is a powerful tool to influence phase change phenomena and related heat transfer. This talk highlights recent advancements from the author's group on electrowetting (EW)-based enhancement and control of boiling, condensation, and freezing.

The first topic is EW-induced suppression [1] of the Leidenfrost state (film boiling), which relies on electrostatic attraction of liquid to the surface. The resulting wettability increase can enhance heat transfer by an order of magnitude and fundamentally change the shape of the classical boiling curve, with very low electrical power consumption. EW can be an enabling tool for tunable boiling hear transfer for liquids such as organic solvents and deionized water. Recent, related fundamental advances from the author's group will be highlighted such as i) the role of AC electric fields on Leidenfrost state suppression [2], ii) Leidenfrost state suppression on liquid substrates [3], and iii) an analysis [4] of the liquid-vapor instability underlying electrostatic suppression. In related research, EW has enabled a novel heat pipe architecture [5] to move high (kiloWatt) heat loads over long distances. An electrowetting heat pipe (EHP) uses EW to pump liquid condensate back to the evaporator, inplace of a wick. This allows the EHP to overcome wick-related capillary pressure limitations on liquid and heat transport. The microfluidics underlying such an EHP was recently characterized on the International Space Station.

The second topic is EW-enhanced condensation [6,7], which enables high condensation rates resulting from rapid condensate removal from surfaces. EW can promote rapid coalescence, growth and shedding/transport of condensed droplets by oscillations/linear translation of condensed droplets. The underlying theory and various modes of operation of EW-enhanced condensation will be discussed.

The third topic is the use of electric fields to promote freezing (electrofreezing) [8], which has applications in the synthesis of natural gas hydrates and ice. The use of electric fields can overcome the induction time barrier for nucleation, and even trigger instantaneous freezing. Electric fields thus provide options for dynamic control of freezing and crystal growth. Overall, this talk will discuss the relevance of EW in the area of phase change, and highlight benefits in the areas of power generation, waste energy utilization, oil-gas production and manufacturing.

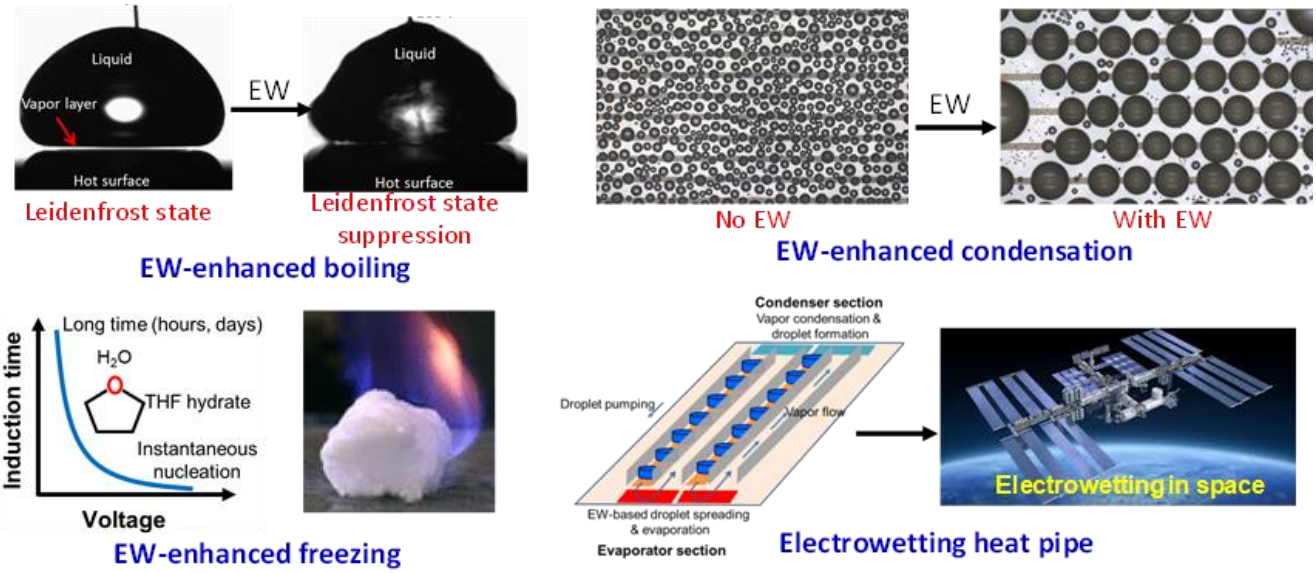

[1] Shahriari A., Hermes M. and Bahadur V. *Applied Physics Letters*, 108, 091607, 2016.
[2] Ozkan O. Shahriari A. and Bahadur V. *Applied Physics Letters*, 111, 141608, 2017.
[3] Shahriari A., Ozkan O. and Bahadur V. *Langmuir*, 33 (46), 13207-13213, 2017.
[4] Shahriari A., Das S., Bahadur V. and Bonnecaze R. *Physical Review Fluids*, 2, 034001, 2017.
[5] Hale R. and Bahadur V. *Journal of Micromechanics and Microengineering*, 27, 075004, 2017.
[6] Baratian D., Dey R., Hoek H., Ende D.V.D and Mugele F. arXiv:1712.03059, 2018.
[7] Alizadeh A., Bahadur V., Kulkarni A., Yamada M. and Ruud J. A. *MRS Bulletin on Interfacial Materials with Special Wettability*, 2013.
[8] Acharya P. and Bahadur V. *Advances in Colloid and Interface Science*, 251, 26-43, 2018.

Electrowetting displays: 15 years and counting

Alex Henzen [1, 2,3], Guofu Zhou [1, 2, 3]

[1]*Guangdong Provincial Key Laboratory of Optical Information Materials and Technology & Institute of Electronic Paper Displays, South China Academy of Advanced Optoelectronics, South China Normal University, Guangzhou, 510006, P. R. China*

[2]*GR8 optoelectronics Ltd, Hong Kong*

[3]*Shenzhen Guohua Optoelectronics Tech. Co. Ltd., Shenzhen, 518110, P. R. China*

Electrowetting displays have been demonstrated since 2004. They have been subject to extensive investigation, and many (but not all) of the problems associated with the electrowetting phenomenon were solved. However, understanding the principle doesn't mean a working, attractive display can be made. Electrowetting displays could (and should) play an important role in a growing collection of display technologies, and will add significantly to our interaction with our environment, but is important to understand exactly how to implement and apply this technology. Maybe even more important: How not to apply it.

One of the challenges of electrowetting displays is the creation of a brightly reflecting color display. There is no obvious point in trying to make an "LCD replacement" and work with backlights, so the factor "reflectance" plays a very important role.
While reflective (monochrome) LCDs can reach almost 50% reflectance, any technology offering an improvement should surely significantly surpass this. Electrowetting displays claim just this. However, there seems to be a catch: Most display examples are configured in such a way that we can only expect 50% – 60% reflectance: only marginally better than LCD. In order to make a difference, reflectance will need to be >80%! This means some radical improvement in today's architecture must be made, and in particular pixel size and dye film thickness play the determining roles (see figure 1).

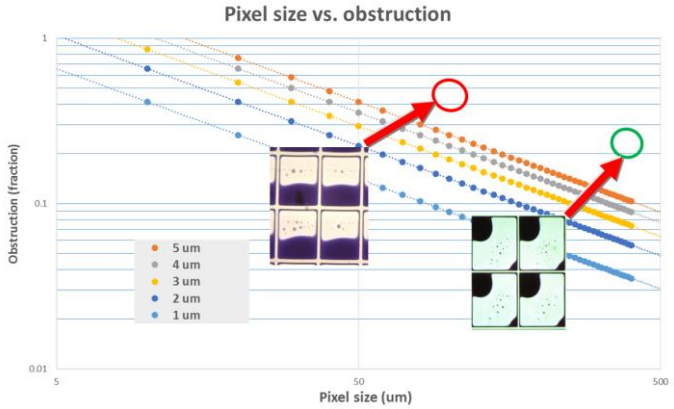

Figure 1: Pixel obstruction vs. size and ink thickness: Simplified theory and practice

Once reflectance is under control, a choice must be made regarding the color system: RGB color filter additive or CMY multi-layer subtractive color. Aperture provides the key to which one is preferred. Surprisingly, this is not a simple choice for one or the other.
The remaining properties to make a useful display are switching speed and power consumption. The former has always been a strong point of electrowetting displays, although controlling the switching flow can be challenging, but control is possible by electrical and mechanical (capillary) means. The latter presents a complex problem, since electrowetting displays need a high voltage to switch, and although a current is not required, keeping the power low puts a high demand on the insulating properties of the insulator.

With most of the problems solved, or at least with a feasible solution within reach, electrowetting displays will soon become a part of the ever growing commercial display family.

This project is supported by National Key R&D Program of China (No. 2016YFB0401501), National Natural Science Foundation of China (No. 61771204), Guangdong Innovative Research Team Program (No. 2013C102), Guangdong Natural Science Foundation (No. 2016A030310438, 2016B090909001), Science and Technology Project of Shenzhen Municipal Science and Technology Innovation Committee (GQYCZZ20150721150406), MOE International Laboratory for Optical Information Technologies and the 111 Project.

Topic no. 8
Oral

EW Conf. 2018

Cybermanufacturing ecosystem for expanding electrowetting community

Jia Li and Chang-Jin "CJ" Kim
University of California, Los Angeles (UCLA), California 90095, U.S.A.

Despite the impressive research progress over the last 15-20 years and recent commercialization, the electrowetting community is still rather small. We suspect two main bottlenecks have been preventing many potential researchers from joining the field: technical barriers and reliability issues, as illustrated in Figure (a). Technical barriers refer to the manufacturing of electrowetting chips or plate, which often requires special resources and knowledge, and the building of control electronics and software to operate them. Reliability issues refer to the major failure mechanisms of the chips or plates during usage, such as the current leakage (short-term failure often manifested as electrolysis) through the dielectric layer and the electric charging (long-term degradation often stalling the electrowetting effect) of the hydrophobic topcoat on the electrowetting-on-dielectric (EWOD) chip. In an effort to widen the above bottlenecks, we propose to build a cybermanufacturing system which will cultivate an ecosystem where a wide range of users (e.g., researchers, entrepreneurs, students, hobbyists) can focus on their own ideas and applications without worrying about the engineering and manufacturing side of electrowetting technology.

Supported by the U.S. National Science Foundation (NSF), our current plan is to build a cybermanufacturing system that resides on a cloud server. Via a portal website, a user can access 5 major web services that link (i) users, (ii) CAD providers, (iii) operating system providers, (iv) EWOD chip foundries, and (v) online community, as illustrated in Figure (b). The first web service is for the users. User can create online profile which reloads their preferred settings and saved work once they log in. The second web service is an online CAD[1,2] to assist designing electrowetting chips and plates. Instead of the typical practice of users drawing mask file from scratch, the electrowetting CAD provides typical electrode shapes and arrangements for the users to simply drag and drop and generates the custom mask file that meets design rules. The third web service is an ecommerce-type platform where the user can obtain the control system[3,4,5] online. In addition to the basic operating system, we envision add-on systems for more functionality, such as heating and magnetic actuation. The fourth web service is foundries who receive chip design file from the users and fabricate chips and plates[6] for them. Different users share the same fabrication process using only standard materials and specifications in a way printed circuit board (PCB) business is run today. This limitation is necessary is to keep the cost under control and ensure device reliability. One would lose the freedom in chip design and device configuration significantly but in return receive working product with little effort. The combination of a pre-made control system and the foundry service ensure users encounter minimal reliability issues during experiments. The fifth web service provides an online community, where users share their own chip design file and build on others'. An internet forum is included for support and discussion among the users.

The online cybermanufacturing described above requires some hardware and services available offline. At this point, we have prototyped a compact control system that is versatile and user-friendly. The control system is being stress-tested to make it more reliable and safe for public users. For CAD, we are incorporating auto electrode layout and routing algorithms. For the chip fabrication, we need to establish a reliable fabrication process and transfer it to a willing foundry. In sum, we propose the concept of cybermanufacturing ecosystem to lower the technical barriers and allow researchers from various background and even public to exercise electrowetting. With a larger community, we have more chance to overcome existing limitations and spark innovative applications. Meanwhile, this system provides a port for the industry (CAD companies, instrument manufacturers, and chip foundries) to contribute to this field.

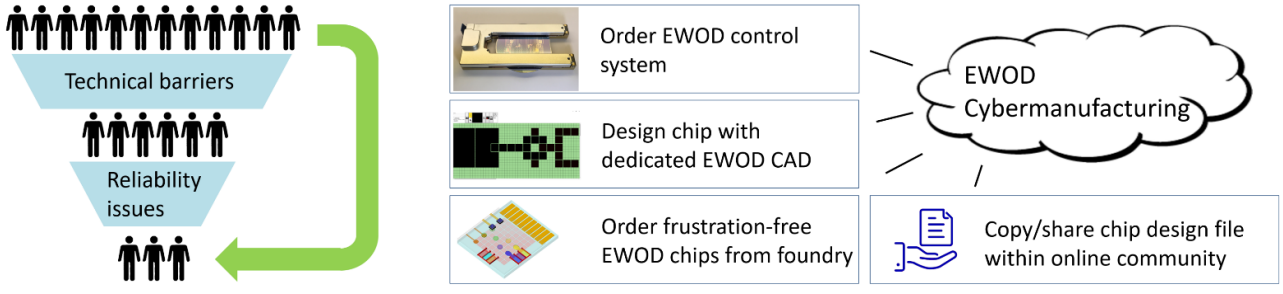

Figure. (a) Technical barriers and reliability issues hinder potential researchers from joining electrowetting. (b) The cybermanufacturing provides an ecosystem for users in mass to perform electrowetting.

Reference:

[1] Chen, Ying-Han, et al. IEEE TCAD, vol. 32, pp. 1151-1162 (2013).
[2] Wang, Qin, et al. ICCAD, vol. 103 (2016).
[3] J. Li and C.-J. Kim, Proc. microTAS, Gyeongju, S. Korea, pp. 1199-1201 (2015).
[4] Fobel, Ryan, Christian Fobel, and Aaron R. Wheeler. Applied Physics Letters vol. 102, pp.193513 (2013).
[5] http://www.gaudi.ch/OpenDrop/?p=17I
[6] Ko, Hyojin, et al. Advanced Materials vol. 26, pp. 2335-2340 (2014).

Energy harvesting using novel microfluidic liquid metal homopolar generator

Karan Panchadar, Devin West, J. Ashley Taylor, and Tom Krupenkin
University of Wisconsin – Madison, Madison, WI, USA

A novel mechanical to electrical energy conversion method has been proposed and experimentally demonstrated. The method employs a circular swirling flow of a conductive liquid metal (mercury or Galinstan) through a cylindrical cavity in the presence of high strength magnetic field. The schematic outline of the device is shown in Fig. 1 (a) and the developed liquid flow pattern is shown in Fig. 1 (b). Similar to traditional homopolar generators the voltage differential between the center and the periphery of the flow chamber is developed due to the presence of the Lorentz force acting on the electrons in the moving electrical conductor. However, unlike the traditional homopolar generator the developed device has no moving mechanical parts which greatly simplifies the system design and substantially improves its performance.

The system behavior was investigated both experimentally and theoretically. The generated voltage was measured as a function of electrical load, magnetic field strength and the flow velocity. A simple theoretical model, which describes the device operation, was developed and found to be in good agreement with the experimental data as shown in Fig. 1 (c). This new approach is potentially capable of providing high power density and is well suited for converting mechanical energy from a multitude of environmental energy sources characterized by a wide range of forces and displacements.

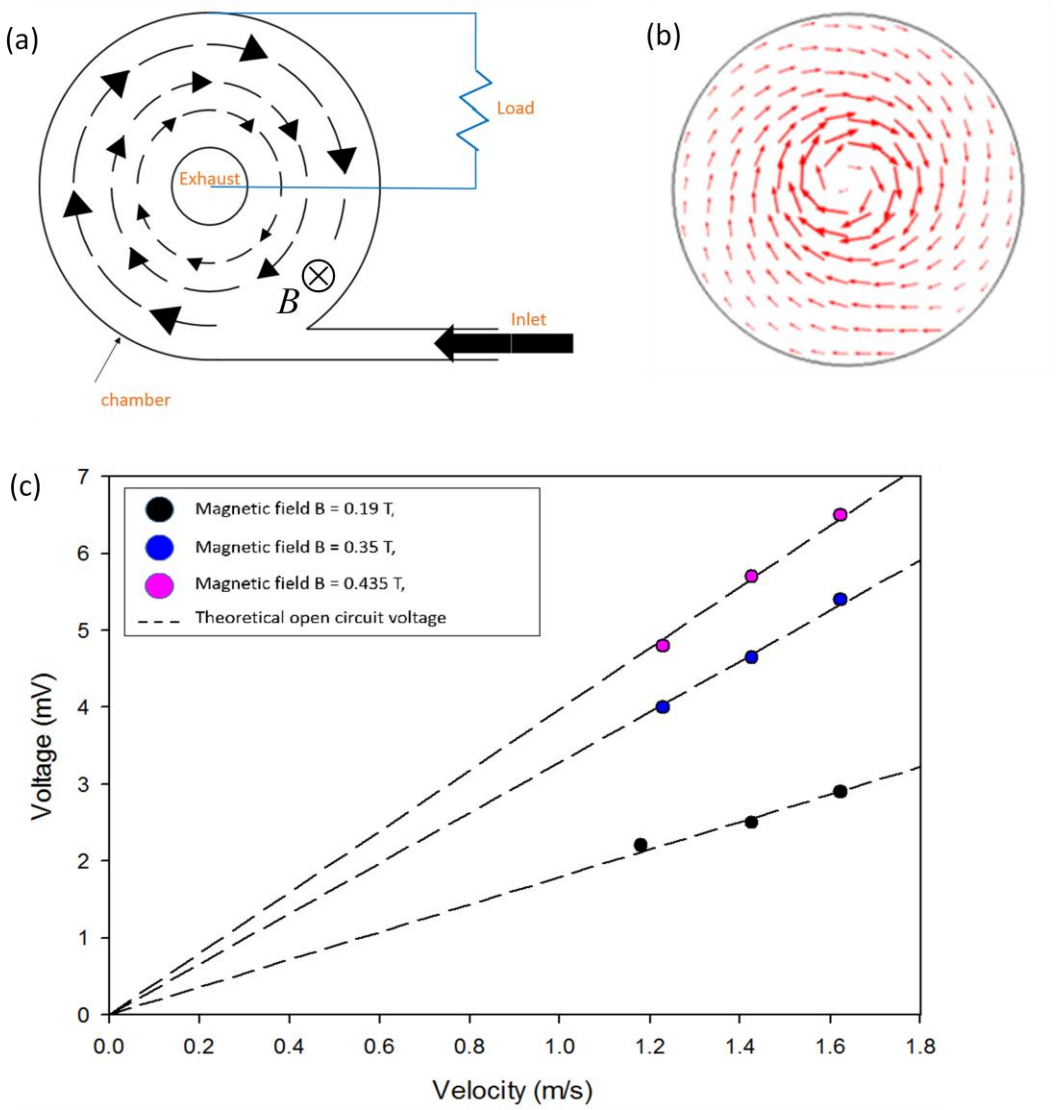

Fig. 1 (a) Schematic outline of the liquid homopolar generator. (b) Flow velocity pattern developed in the homopolar generator chamber. (c) Voltage generated between the center and the periphery of the chamber as a function of the inlet flow velocity and the magnetic field strength. Dashed lines represent the theoretical model prediction.

Dynamics of oscillations and coalescence of compound droplets by AC electrowetting

Shubhi Bansal [1] and Prosenjit Sen [1]
[1] *Centre for Nano Science and Engineering, Indian Institute of Science*
shubhib@ iisc.ac.in

Manipulation of compound droplets on planar substrate facilitates the use of complex and biological fluids for different lab on chip applications [1]. Compound droplets, formed by encapsulating sample core in an oil shell, reduces sample contamination, evaporation and contact line hysteresis [2]. The oscillations of compound droplets using low frequency (< 200Hz) AC electrowetting [3] exhibits axisymmetric and non-axisymmetric modes. The dynamics of these oscillations were found to be affected by the shell volume. We have studied the use of these oscillations for applications like enhancing on-chip mixing. On-chip mixing however requires coalescence of the two droplets which was found to be affected by the interface dynamics of the two oscillating compound droplets. We investigated the interaction between two droplets placed adjacent to each other in an oil shell and oscillated by low frequency AC electrowetting as shown in Figure 1a. Coalescence of droplets on oil infused surfaces had been investigated earlier with [4] and without [5] voltage based on electro-coalescence, which is avoided here by applying voltage of same magnitude and phase to both the core droplets. We observed that without oscillations the core droplets merged rapidly (< 10s) as shown in Figure 1b, however, by oscillating droplets with certain actuation parameters, stable non-coalescence (> 80s) was achieved as shown in Figure 1c. The transition from coalescing to non-coalescing regime was explained based on mode amplitude of the core-shell interface, evolution of entrapped oil bridge between cores and other viscous - capillary forces. The parameters affecting coalescence of the oscillating droplets like the actuation parameters, core and shell properties like viscosity and droplet size, were also examined.

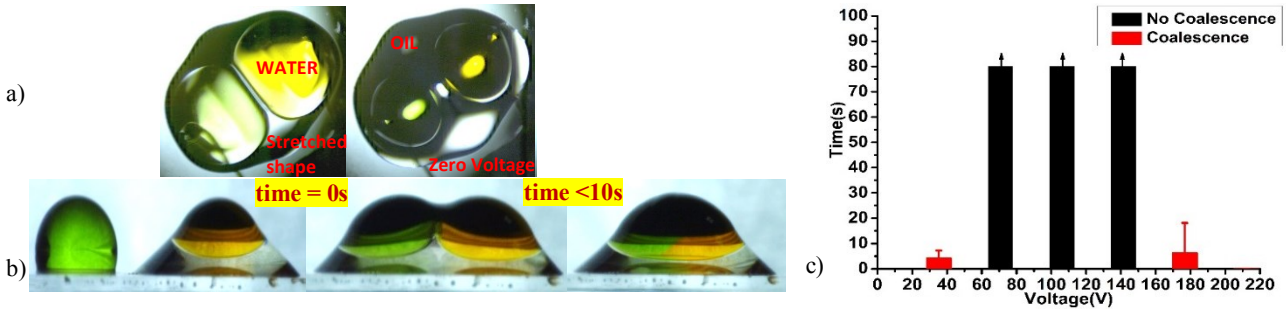

Figure 1: a) Bottom view images demonstrating oscillations of two core water droplets in oil shell using AC electrowetting with 106V_{rms} actuation voltage at 25Hz. The core droplets show oblate/prolate stretching during maximum voltage and goes to spherical cap shape with nearly circular contact line during zero voltage. b) Side view images showing droplet coalescence without actuation. c) The observed time taken for coalescence of core water droplets during oscillations with different actuation voltages at 25Hz by AC electrowetting. The black portion marks the captured non-coalescence time limit (~80s) and the arrows above it show that no coalescence continues even after this limit.

References

1. Li, J., Wang, Y., Chen, H. and Wan, J., *Lab Chip* **14,** 4334–7 (2014).
2. Brassard, D., Malic, L., Normandin, F., Veres, T. and Tabrizian, M., *Lab Chip* **8,** 1342–9 (2008).
3. Bansal, S. and Sen, P., *Langmuir* **33**, 11047-11058 (2017).
4. Barman, J., Nagarajan, A. K. and Khare, K., *RSC Adv.* **5,** 105524–105530 (2015).
5. Boreyko, J. B., Polizos, G., Datskos, P. G., Sarles, S. A. and Collier, C. P., *Proc. Natl. Acad. Sci.* **111,** 7588–7593 (2014).

Fundamental Challenges in Molecular Modeling of Electrowetting

Alenka Luzar
Department of Chemistry, Virginia Commonwealth University, 1001 West Main Street, Richmond, VA 23284-2006

Interfacial phenomena play a determining role in macroscopic behavior of complex materials systems and devices. Interfacial properties can often be manipulated by the application of external fields. The talk will review our recent simulation advances toward understanding on a molecular scale how one can control ion adsorption to hydrophobic surfaces in electric fields, salt partitioning, wetting free energy, and dynamic responses in electrically controlled systems.

Electroprewetting in pores: filling transition and chemical reaction

Sela Samin[1], Shivaraj Deshmukh[2], and Yoav Tsori[2]
[1]*Institute for Theoretical Physics, University of Utrecht, the Netherlands*
[2]*Department of Chemical Engineering, Ben-Gurion University of the Negev, Israel*

We examine theoretically 'electroprewetting' transitions in porous membranes. In aqueous mixtures, we show that the membrane's pores can be reversibly gated from `off' (co-solvent-rich, poor conductor of ions and other solutes) to 'on' (water-rich, good conductor) states by an external potential [1]. The transition voltage or charge for switching depends on the membrane hydrophilicity/hydrophobicity, the salt content, the preferential solvation of the salt ions, and the temperature. These parameters also determine whether the filling transition is first or second order.
We further look at chemical reactions taking place in such mixtures. We show that the filling transition can dramatically accelerate or slow down the reaction [2]. It can be used as a method to control runaway temperature sensitive reactions and to increase the reaction rate without using catalysts, which is especially important in biomedical application.

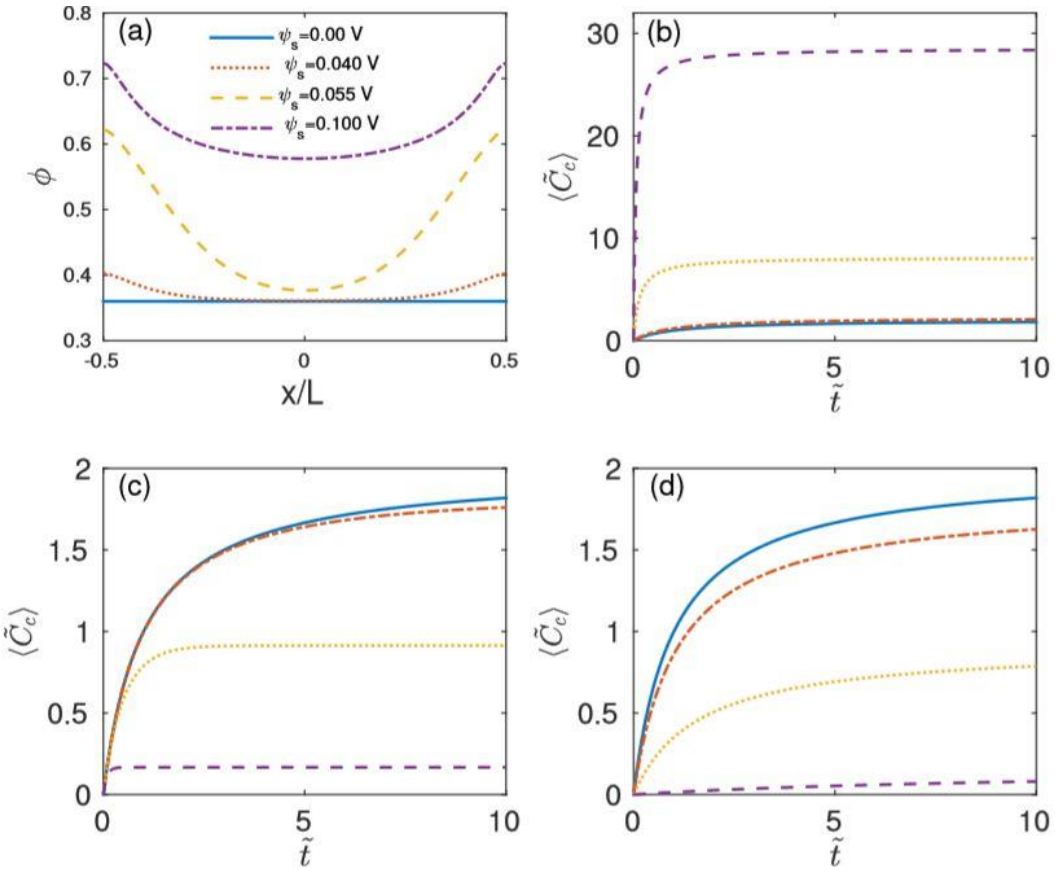

Control of the effective reaction rate in pores using external potentials. The pore is modeled as two parallel flat plates located at x=±L/2 across which potential ψ_s is applied. (a) Profiles $\phi(x)$ for the composition of the polar solvent inside the pore for different electric potentials ψ_s. A filling transition occurs as the pore potential increases. (b) Change in time of the product concentration averaged over the pore volume, $\langle C_c \rangle$. Both reactants A and B are more soluble in the polar phase and the reaction is accelerated. Colors and linestyles correspond to the same values of ψ_s in (a). The concentrations of the molecular species i=A,B at time t=0 was $C_i=C_0\exp(-u^i\phi)$. (c) The same as in (b) but reactant A is polar and reactant B is nonpolar. The reaction is slowed down by the potential. (d) As in (b) but both reactants are nonpolar and the reaction is slowed down by the potential. In all parts we took L=10 nm, ϕ_0=0.36, and T=0.99T_c.

References

[1] S. Samin and Y. Tsori, Reversible pore gating in aqueous mixtures via external potential *Coll. Interf. Sci. Comm.* **12**, 9 (2016).

[2] S. D. Deshmukh and Y. Tsori, Control of chemical reactions using electric field gradients J. Chem. Phys. (Communication) **144**, 191102 (2016).

Topic no. XX (see website/flyer)
Oral or poster

EW Conf. 2018

Solvation effects on electrowetting at the nanoscale

Nicolas Rivas[1], Jens Harting[1,2]

[1]*Forschungszentrum Jülich, Helmholtz Institute Erlangen-Nürnberg for Renewable Energy (IEK-11)*
Fürther Straße 248, 90429 Nürnberg, Germany

[2]*Department of Applied Physics, Eindhoven University of Technology*
PO Box 513, 5600MB Eindhoven, The Netherlands

Electrowetting of nanoscopic sessile drops is studied for aqueous electrolyte mixtures. We find that the relative ion concentration between the solvents, determined by the Gibbs transfer energy, controls both the amount and the maximum attainable deformation of the drop, as shown in Fig. 1. An expression is given, based on the electrokinetic equations, for the dependency of the drop's contact angle with the ion concentration and the strength of the solvation potential in the absence of external electric fields, showing good agreement with numerical solutions of the electrokinetic model [1]. As in classical electrowetting experiments contact angle saturation is observed [2], where the contact angle increases with the applied electric field only until a given point. Saturation is traced to be driven by the depletion of ions from the drop and therefore controllable via the Gibbs transfer energy, a finding of possible practical significance.

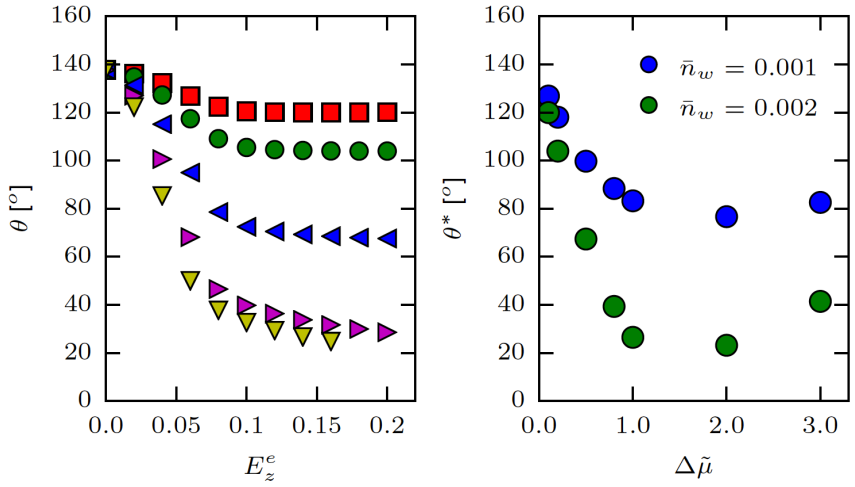

Figure 1. (left) Sessile drop contact angle θ as a function of the applied external electric field E_z^e in simulation units, for different dimensionless Gibbs transfer energies $\Delta\mu = -0.1$ (□), $\Delta\mu = -0.2$ (○), $\Delta\mu = -0.5$ (▷), $\Delta\mu = -1.0$ (◁) and $\Delta\mu = -2.0$ (▽) for a drop ion concentration of 2 mM. (right) Minimum contact angle attainable θ^* as a function of $\Delta\mu$ and different drop ion concentrations $\bar{n}_w$.

[1] F. Capuani, I. Pagonabarraga, and D. Frenkel, The Journal of Chemical Physics **121**, 973 (2004).
[2] S. Chevalliot, S. Kuiper, and J. Heikenfeld, Journal of Adhesion Science and Technology **26**, 1909 (2012).

Electrowetting as a probe for surface chemistry of materials

B. Manchon[1], G. Bonfante[1], M. Maillard[1]
[1]*Université de Lyon, Université Claude Bernard LYON1, Laboratoire des Multimatériaux et Interfaces, UMR CNRS 5615, F-69622 Villeurbanne, France*

Abstract

For many applications including electrowetting actuated devices, understanding interaction between hydrophobic coatings and chemical environment is of critical importance to optimize both performances and reliability [1,2].
The objective of this work is use polarization mechanisms at the interface between a dielectric coating, an electrolyte and an insulating liquid, to probe chemical surface properties from the hydrophobic coating.
We performed electrowetting under DC and modulated DC voltage [3], while modifying the chemical environment of the hydrophobic layer.
We observed instantaneous and drastic modifications of the electrowetting actuation, as a non-symmetric response to positive and negative bias while modifying chemical environment. We demonstrate for example that controlling pH from electrolyte induces a reversible modification of hydrophobic properties from coatings, and in the case of a partially oxidized materials, a restauration of hydrophobic properties is obtained.
This approach has proven to be successful to probe surface chemistry from hydrophobic coatings in their chemical environment and electrowetting actuation is advantageously used as a surface analysis tool.

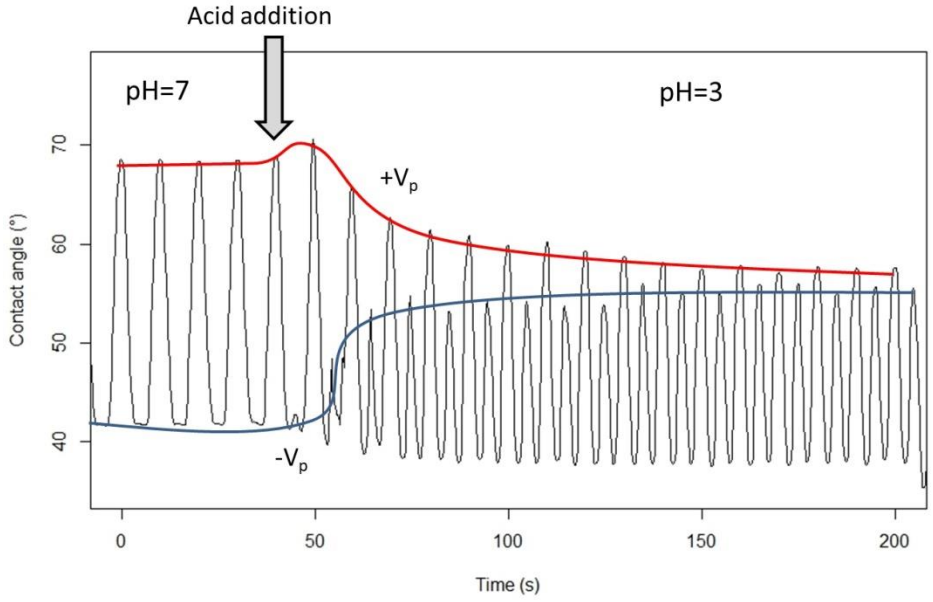

Figure caption: Electrowetting actuation of dodecane under modulated DC voltage during acid addition, observed on a 7µm thick parylene C at ±60V 0.1Hz

[1] Bonfante, G.; Maillard, M.; Chevalliot, S.; Burger, B.; Berge, B.; Gablin, C.; Leonard, D.; Toury, B. Failure Mode Analysis on Thermally Aged Hydrophobic Coatings Applied to Electro Wetting. *Thin Solid Films*, **646**, 53–60 (2018)

[2] Banpurkar, A. G.; Sawane, Y.; Wadhai, S. M.; Murade, C. U.; Siretanu, I.; Ende, D. van den; Mugele, F. Spontaneous Electrification of Fluoropolymer–water Interfaces Probed by Electrowetting. *Faraday Discuss.*, **199**, 29–47 (2017)

[3] Bonfante, G.; Roux-Marchand, T.; Audry-Deschamps, M.-C.; Renaud, L.; Kleimann, P.; Brioude, A.; Maillard, M. Polarization Mechanisms of Dielectric Materials at a Binary Liquid Interface: Impacts on Electrowetting Actuation. *Phys. Chem. Chem. Phys.*, **19**, 30139–30146. (2017)

Poster list

Poster no.	Title	Authors
P1	Thickness dependence on the wettability of thin films	F. Foadi; M. R. Mohammadizadeh; S.M. Vaez Allaei
P2	Contact Angle Hysteresis and Phase Angle Effect on Forces in Electrowetting on Dielectric Microfluidic Device	Matin Torabinia; Ali Farzbod; Arvind Venkatesan; Hyejin Moon
P3	A Holistic Review of Wetting of Droplets	Jennifer Dodoo; Mohammed E. Sayed; Logan Mackay; Glen McHale; Adam A. Stokes
P4	Formation of Droplet Jet by Enhanced Condensation of a Heated Drop Subjected to AC Electric Field	Krishnadas; Narayanan Nampoothiri; M.S. Bobji; Prosenjit Sen
P5	Investigation of movements and particle velocity induced by EWOD inside droplets of different viscosities	Marta Podrażka; Annelies Voorhaar; A. Robert Hillman; Karl S. Ryder; Martin Jönsson-Niedziółka
P6	Dewetting from a Liquid Film into a Single Droplet in Air and Liquid	Glen McHale; Rodrigo Ledesma-Aguilar; Michael I. Newton; Andrew Edwards; Carl. V. Brown
P7	Contact angle hysteresis and oil film lubrication in electrowetting with two immiscible liquids	Jun Gao, Niels Mendel, Ranabir Dey, Davood Baratian, Frieder Mugele
P8	Dynamics of oscillations and coalescence of compound droplets by AC electrowetting	Shubhi Bansal; Prosenjit Sen
P9	Printing of functional material inks to modify surface wettability in paper-based microfluidic chips	Veasna Soum; Yunpyo Kim; Mary Chuong; Sooyong Park; Oh-Sun Kwon; Kwanwoo Shin
P10	Low-Voltage EWOD Investigated by Electrical Impedance Spectroscopy	Ying-Jia Li; Brian P. Cahill
P11	Digital Microfluidics Platform for DNA Data Storage	Ashley P. Stephenson; Sharon Newman; Max Willsey; Bichlien H. Nguyen; Christopher N. Takahashi; Karin Strauss; Luis Ceze
P12	Recent progress towards a worn biodetector	L. Coudron; T. Foat; M. McDonnell; D. McCluskey; I. Munro; I. Johnston; C. Tan; W. Sellors; D. Despeyroux; M. Tracey
P13	A Novel Electrode design for Efficient Droplet actuation using EWOD	Mainak Basu; Soumen Das; Sunando DasGupta
P14	Electrowetting on dielectric: history effects on rupture voltage	Qing Zhao; Biao Tang; Jan Groenewold; Guofu Zhou
P15	Electrowetting droplet manipulation at -30 to 80 C for optical applications	Sandip M. Wadhai; Arun G. Banpurkar
P16	Highly hydrophobic copper based microcrystalic surfaces prepared by electrodeposition method	Raziyeh Akbari; Mohammadreza Mohammadizadeh; Gabriela Ramos Chagas; Guilhem Godeau; Frédéric Guittard; Thierry Darmanin

P17	Modelling of Electrowetting and Other Interfacial Properties of Liquids on Graphene	Jezabel Boni; Paola Carbone; Robert Dryfe; Anne Juel
P18	Low Voltage Electrowetting on Ferroelectric PVDF-HFP Insulator	Sandip M. Wadhai; Yogesh B. Sawane; Anurag Kanase; Arun G. Banpurkar
P19	Electrowetting-based Rapid Coalescence and Growth of Droplets for Condensation Enhancement	Enakshi D. Wikramanayake; Vaibhav Bahadur
P20	Using EWOD systems for microfluidic digital patterning	Hsiang-Ting Lee; Da-Jeng Yao
P21	Pyro-electrification of polymer membranes for multipurpose applications	Romina Rega; Oriella Gennari; Laura Mecozzi; Simonetta Grilli; Vito Pagliarulo; Pietro Ferraro
P22	The pyro-electrowetting enables the actuation of compliant micro-bumps into a skin-over-liquid platform	O. Gennari; R. Rega; L. Mecozzi; V. Pagliarulo; A. Bramanti; P. Ferraro; S. Grilli
P23	Integration of micro heater and sensor on paper-based DMF chip by using material inkjet printer	Yunpyo Kim; Veasna Soum; Mary chuong; Sooyong Park; Oh-Sun Kwon; Kwanwoo Shin
P24	Micro/bio-object manipulation by AC-EWOD driven twin bubbles	Jeong Byung Chae; Kang Yong Lee; Jeongmin Lee; Dae Geun Kim; Sang Kug Chung
P26	Bending of elastic pillars using electric field: The influence of electrowetting	Arvind Arun Dev; Ranabir Dey; Frieder Mugele
P28	Charge trapping in fluoropolymer under electrowetting	Hao Wu; Igor Siretanu; Dirk van den Ende; Frieder Mugele

Instructions for participants:

1. Welcome drinks will be at Hotel the Drienerburght on **Sunday June 17th, 18.00-20.00 hrs**. (see map buildingnr.44 at Campus). **Registration will be possible during the welcome drinks.**

2. For arriving at the university from the station: from Enschede Central Station take either bus 1 or bus 9 to Universiteit; from Enschede Kennispark take bus 1 to Universiteit.

3. For directions from the hotel to the conference auditorium, please see the map at the back of the program (also attached herewith for convenience).

4. **Monday June 18, Check in / Registration at Hal B**. There will be lockers available equipped with a charging point for your mobile. For the last day of the Conference there is a room available (2E) at Hal B for safely storing your luggage. Just ask for the key at the service desk in Hal B.

5. The nearest restaurant is at Hotel de Broeierd. Otherwise, several restaurants are present between the train station and the Old Market in Enschede City Centre.

6. All Conference volunteers will be wearing purple polo shirts.

7. **Wi-fi:** eduroam (if you have an account); for those who do not have accounts- UTGUEST; Enschede_Stad_Van_Nu

8. In case of Emergency: dial +31534892222

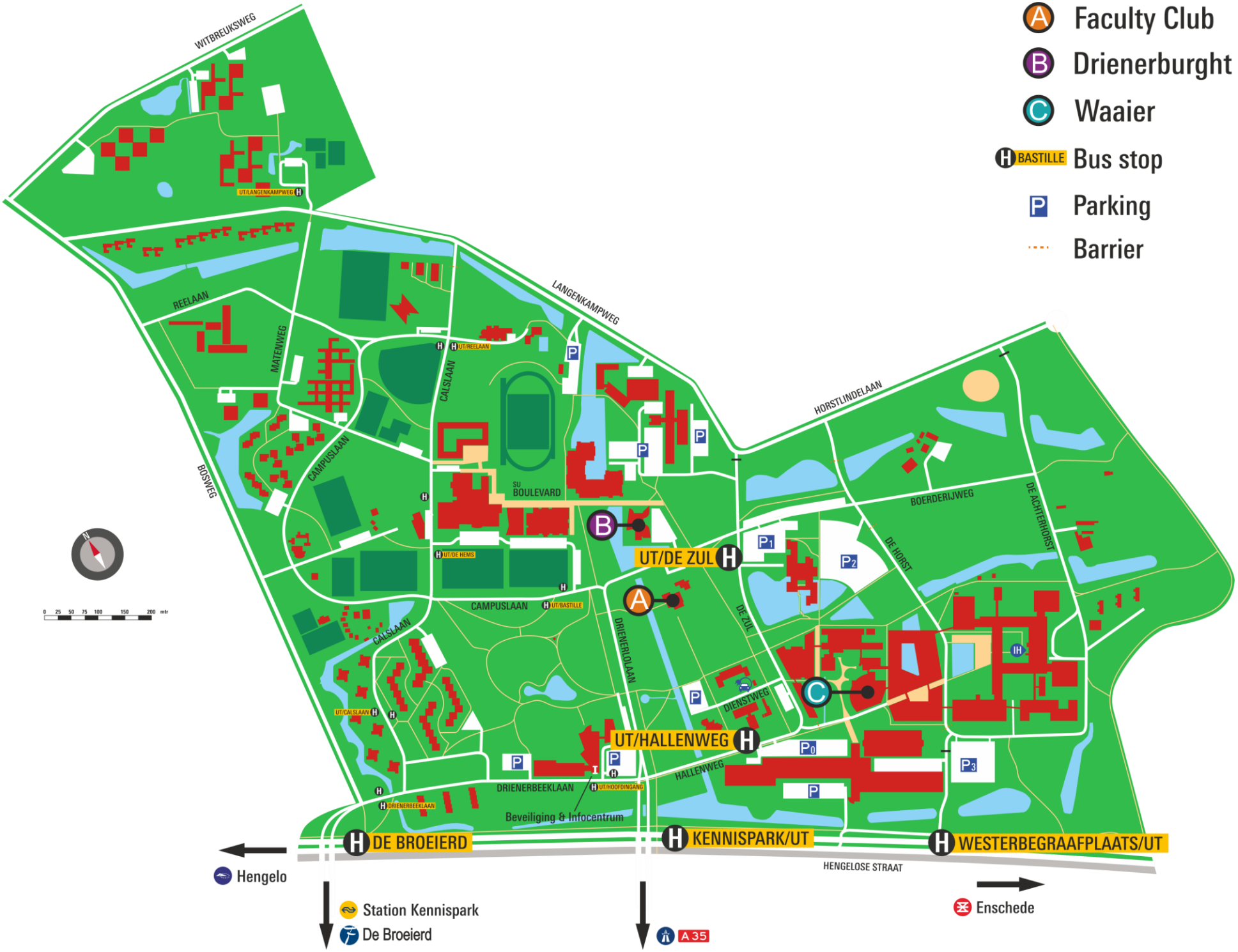
Faculty Club
Drienerburght
Waaier
BASTILLE Bus stop
Parking
Barrier
WITBREUKSWEG
UT/LANGENKAMPWEG
REELAAN
MATENWEG
LANGENKAMPWEG
HORSTLINDELAAN
UT/REELAAN
CALSLAAN
CAMPUSLAAN
BOSWEG
SU BOULEVARD
BOERDERIJWEG
DE ACHTERHORST
DE HORST
UT/DE HEMS
UT/DE ZUL
CAMPUSLAAN
UT/BASTILLE
CALSLAAN
DRIENERLOLAAN
DE ZUL
DIENSTWEG
UT/CALSLAAN
UT/HALLENWEG
HALLENWEG
DRIENERBEEKLAAN
UT/HOOFDINGANG
DRIENERBEEKLAAN
Beveiliging & Infocentrum
DE BROEIERD
KENNISPARK/UT
WESTERBEGRAAFPLAATS/UT
HENGELOSE STRAAT
Hengelo
Station Kennispark
De Broeierd
A 35
Enschede

Supported by